



Cite this: *Sustainable Energy Fuels*, 2020, 4, 2114

## Green hydrogen from anion exchange membrane water electrolysis: a review of recent developments in critical materials and operating conditions

Hamish Andrew Miller, <sup>\*a</sup> Karel Bouzek, <sup>b</sup> Jaromír Hnat, <sup>b</sup> Stefan Loos, <sup>c</sup> Christian Immanuel Bernäcker, <sup>c</sup> Thomas Weißgärtner, <sup>c</sup> Lars Röntzsch and Jochen Meier-Haack<sup>d</sup>

Hydrogen production using water electrolyzers equipped with an anion exchange membrane (AEM), a pure water feed and cheap components such as platinum group metal-free catalysts and stainless steel bipolar plates (BPP) can challenge proton exchange membrane (PEM) electrolysis systems as the state of the art. For this to happen the performance of the AEM electrolyzer must match the compact design, stability, H<sub>2</sub> purity and high current densities of PEM systems. Current research aims at bringing AEM water electrolysis technology to an advanced level in terms of electrolysis cell performance. Such technological advances must be accompanied by demonstration of the cost advantages of AEM systems. The current state of the art in AEM water electrolysis is defined by sporadic reports in the academic literature mostly dealing with catalyst or membrane development. The development of this technology requires a future roadmap for systematic development and commercialization of AEM systems and components. This will include basic and applied research, technology development & integration, and testing at a laboratory scale of small demonstration units (AEM electrolyzer shortstacks) that can be used to validate the technology (from TRL 2–3 currently to TRL 4–5). This review paper gathers together recent important research in critical materials development (catalysts, membranes and MEAs) and operating conditions (electrolyte composition, cell temperature, performance achievements). The aim of this review is to identify the

Received 14th December 2019

Accepted 4th March 2020

DOI: 10.1039/c9se01240k

[rsc.li/sustainable-energy](http://rsc.li/sustainable-energy)

<sup>a</sup>*Istituto di Chimica dei Composti Organometallici (CNR-ICCOM), Via Madonna del Piano 10, 50019 Sesto Fiorentino, Firenze, Italy. E-mail: hamish.miller@iccom.cnr.it*

<sup>b</sup>*University of Chemistry and Technology, Prague, Department of Inorganic Technology, Technická 5, 166 28, Prague 6, Czech Republic*

<sup>c</sup>*Fraunhofer Institute for Manufacturing Technology and Advanced Materials IFAM, Branch Lab Dresden, Winterbergstraße 28, 01277, Dresden, Germany*

<sup>d</sup>*Leibniz-Institut für Polymerforschung Dresden e.V., Hohe Straße 6, D-01069 Dresden, Germany*



Hamish Andrew Miller is a researcher at the ICCOM institute of the CNR based in Florence, Italy. After receiving his PhD in inorganic chemistry from the Queen's University of Belfast (UK) in 1999, he spent 10 years working in the chemical industry including 6 years developing fuel cells and electrolyzers. His major research interests involve nanotechnology and electrocatalysis in energy

related fields. In particular developing PGM-free electrocatalysts for alkaline anion exchange membrane fuel cells and electrolyzers, electroreforming of renewable alcohols for co-production of chemicals and hydrogen and investigating the electrochemical reduction of CO<sub>2</sub> to fuels and chemicals.



Karel Bouzek obtained his PhD from the University of Chemistry and Technology, Prague and currently he acts at the same University as a full professor at the Department of Inorganic Technology. His primary focus is on electrochemical engineering and technical electrochemistry. Currently he deals predominantly with hydrogen related processes, i.e. fuel cells and water electrolyzers, including alkaline ones. Beside experimental study, his activities involve also the topic of mathematical modelling of electrochemical systems.



current level of materials development and where improvements are required in order to demonstrate the feasibility of the technology. Once the challenges of materials development are overcome, AEM water electrolysis can drive the future use of hydrogen as an energy storage vector on a large scale (GW) especially in developing countries.

## 1. Introduction

Hydrogen is a vital raw material used in industries such as ammonia synthesis for fertilisers, metallurgical reduction for steel refining and in the processing of crude oil.<sup>1,2</sup> At present, globally around 70 Mt<sub>H2</sub> per year are used in a pure form while a further 45 Mt<sub>H2</sub> are used in industry without prior purification from other gases. H<sub>2</sub> has long been proposed as an alternative energy vector to fossil fuels to generate power for domestic heating,<sup>3,4</sup> industrial<sup>5</sup> and transport sectors.<sup>6–10</sup> In this sense, it has the potential to revolutionize the world's energy economy towards the predicted hydrogen economy/society.<sup>9,11,12</sup> Hydrogen is contained in water and in hydrocarbons and is one

of the most abundant elements available on our planet. It can be produced by a variety of methods (thermal, electrolytic and photolytic) from various sources like hydrocarbons, water or biomass. By far the most common method is steam reforming of methane or other hydrocarbons, which causes significant CO<sub>2</sub> emissions. On the other hand, water electrolysis is a well-established mature technology used in special applications. Recently, H<sub>2</sub> has been used to exploit renewable energy (wind, solar) to produce H<sub>2</sub> as energy vector for grid balancing or power-to-gas and power-to-liquid processes.<sup>13–16</sup> There are two main water electrolysis technologies that produce H<sub>2</sub> at low temperatures, which can be distinguished by the electrolyte used in the electrolysis cell: alkaline electrolysis (AE) and proton exchange membrane (PEM) electrolysis. Additionally, the solid



*Jaromír Hnat finished his PhD in Inorganic technology at the University of Chemistry and Technology in Prague (UCTP) in 2015. Currently, he is in the position of Professor assistant at the Department of Inorganic Technology at UCTP. His research focuses primarily on the alkaline water electrolysis, particularly catalyst synthesis, anion exchange membrane testing, membrane electrode assembly preparation, cell and stack design and their characterisation. He is active in the field of the alkaline fuel cells, too.*



*Christian Immanuel Bernaecker received his PhD in Chemistry from Julius-Maximilians-Universität Würzburg (Germany) in 2011 supervised by Professor Christoph Lambert. The topic of the thesis was Physical Properties of Chromophore Functionalized Gold Nanoparticles. In 2011, he joined the Hydrogen Technology group of Dr Lars Röntzsch at the Fraunhofer Institute for Manufacturing Technology and Advanced Materials IFAM in Dresden. Currently, the main research topics are applied electrochemistry and developing of scalable production routes for electrodes.*



*Stefan Loos received his PhD in Physical Chemistry from Freiberg University of Mining and Technology in 2015 supervised by Professor Florian Mertens working on LiFePO<sub>4</sub> cathodes for lithium ion batteries. As a post-doctoral researcher he did three years of research on catalytically active transition metal oxides/hydroxides for water oxidation in the group of Professor Holger Dau at Free University Berlin investigating catalytic mechanisms and catalyst structures by spectroelectrochemical methods. Currently he is doing applied research on electrode manufacturing and development at Fraunhofer IFAM in Dresden with focus on alkaline electrolysis and membrane electrolysis.*



*Dr Jochen Meier-Haack received his PhD in polymer chemistry from Hamburg University in 1992. He joined the Leibniz-Institut für Polymerforschung Dresden (IPF) in 1993 and became member of the membrane group in 1996. Since 2000 Jochen has been head of the Polymeric Membrane Materials group. His research interests are surface modification for fouling mitigation of membranes used in water treatment and development of ion-exchange membranes (AEM and CEM) for electrochemical applications (fuel cells, water electrolyzers).*



oxide high-temperature steam electrolysis is being developed due to the low cell voltages required, which would be especially useful if the required heat can be used from other exothermic industrial processes.

## 2. Established water electrolysis technologies

### 2.1 Alkaline electrolysis

Alkaline electrolysis is a mature technology for H<sub>2</sub> production up to the MW scale, and represents the most widely used electrolytic technology on a commercial level worldwide.<sup>13,17,18</sup> The AE cell consist of two electrodes (anode and cathode) immersed in a highly concentrated aqueous alkaline electrolyte consisting of 20 to 30 mass% KOH. In traditional AE, the most commonly used anode and cathode materials are low-cost steel or nickel alloy-plated steel materials. The two electrodes are arranged in a zero-gap (or quasi zero-gap) formation using a thin diaphragm, which enables separation of the product gases. The diaphragm is permeable to hydroxide ions and water. Major challenges associated with AE are the handing of the corrosive electrolyte and limited current densities due to moderate OH<sup>-</sup> mobility. Furthermore, the diaphragm does not completely prevent the cross-over of gases from one half-cell to the other. The diffusion of oxygen into the cathode compartment reduces the efficiency of the electrolyser, reacting with the hydrogen present on the cathode side to form water. Additionally, extensive mixing (particularly hydrogen diffusion to the O<sub>2</sub> evolution half-cell) also occurs and must be avoided for safety aspects. This is particularly problematic at low loads (<40%) where the O<sub>2</sub> production rate decreases, thus increasing the H<sub>2</sub> cross-over concentration to dangerous levels (lower explosion limit >4 mol% H<sub>2</sub>).

### 2.2 PEM electrolysis

Proton exchange membrane (PEM) water electrolysis is young technology that has good performance and stability and has established itself in the market place in certain niche applications. In PEM electrolysis, the anode and cathode catalysts are typically IrO<sub>2</sub> and Pt, respectively. An acidic membrane is used as solid electrolyte (perfluorosulfonic acid membranes) instead of a liquid electrolyte (Fig. 1). The membrane conducts H<sup>+</sup> cations from the anode to the cathode and separates the H<sub>2</sub> and O<sub>2</sub> produced in the reaction. PEM electrolyzers generally operate at a current density of 2 A cm<sup>-2</sup> at 50–80 °C and approx. 2.1 V. The kinetics of the hydrogen evolution reaction (HER) in PEM electrolysis are faster than in alkaline electrolysis due to the low pH of the electrolyte and the high active metal surface of Pt electrodes. PEM electrolysis is also safer due to the absence of any caustic electrolyte. An additional advantage of PEM electrolysis is the possibility of using high pressure on the cathode side, while the anode can be operated at atmospheric pressure. The corrosive acidic cell operation environment requires the use of specialised materials. These materials must not only resist the harsh corrosive low pH condition, but also sustain the high applied over voltage at the anode (2 V), especially at high

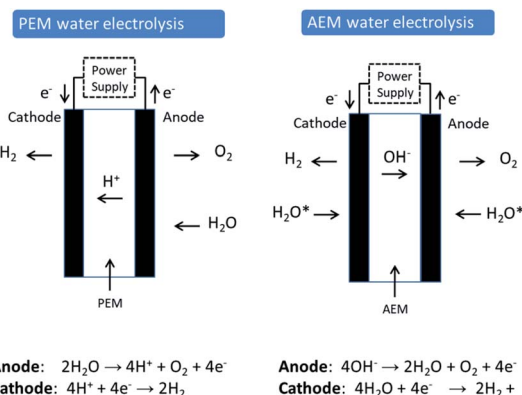


Fig. 1 Comparison of water electrolysis cells and chemistries using either a Proton Exchange Membrane (PEM) or an Anion Exchange Membrane (AEM).\* Current AEM electrolyzers use a water feed with added electrolyte (HCO<sub>3</sub><sup>-</sup>/CO<sub>3</sub><sup>2-</sup> or dilute KOH) to obtain sufficient performance. AEM electrolyzers can operate with electrolyte feed at both electrodes or in anode feed only mode.

current densities. Corrosion resistance applies not only for the catalysts used, but also for current collectors and separator plates. Only a few materials can be selected that can perform in this harsh environment. This demands the use of scarce, expensive materials and components such as noble metal catalysts (e.g. platinum group metals (PGM) like Pt, Ir and Ru), Ti-based current collectors, and separator plates. Ir is one of the rarest elements in the Earth's crust, having an average mass fraction of 0.001 ppm in the Earth's crust (annual production of some tons only). Moreover, Ir use has recently increased due to its use in crucibles employed to fabricate LEDs for smartphones, tablets, televisions and automobiles. It can be expected that production of high volumes of PEM electrolysis units will considerably affect the demand for Ir and consequently the price.

The principle difference between the two technologies (PEM and AE) lies in the significantly higher current densities achievable by a PEM electrolyser that leads to higher production rates and more compact systems (see Table 1 for comparison). To achieve this high loadings of rare and expensive metals for catalysts and expensive corrosion resistant components such as bipolar plates based on high-quality Ti are required.

AEM electrolyser technology, which is discussed in detail in this review, aims at combining the advantages of PEM (membrane separation, pure water feed) with the advantages of AE (cheap and abundant materials).

### 2.3 AEM electrolysis

The concept of AEM water electrolysis has been the subject of various reports in recent years in the academic literature although emphasis has been predominantly on the development of catalyst materials rather than AEM membranes or ionomers. There are very few reports on actual AEM water electrolysis cell performance especially when deionized water is used instead of liquid aqueous KOH. A search of the academic literature (Web of Science) with the words "anion exchange



Table 1 Comparison of the main characteristics of alkaline, PEM and AEM water electrolysis

	Alkaline	PEM	AEM
Electrolyte	Aqueous KOH (20–40 wt%)	Proton exchange ionomer (e.g. Nafion)	Anion exchange ionomer (e.g. AS-4) + optional dilute caustic solution
Cathode	Ni, Ni–Mo alloys	Pt, Pt–Pd	Ni and Ni alloys
Anode	Ni, Ni–Co alloys	RuO <sub>2</sub> , IrO <sub>2</sub>	Ni, Fe, Co oxides
Half-cell separation	Diaphragm (Zirfon Perl 500 µm)	Nafion 117 (e.g. 180 µm)	AEM (20–100 µm)
Current density (A cm <sup>−2</sup> )	0.2–0.4	0.6–2.0	0.2–1.0
Cell voltage (V)	1.8–2.4	1.8–2.2	1.8–2.2
Cell area (m <sup>2</sup> )	<4	<3	Lab testing cells
Operating temperature (°C)	60–80	50–80	50–60
Operating pressure (bar)	1–30	30–76	1–30
Production rate (Nm <sup>3</sup> h <sup>−1</sup> )	<760	<40	<1
Gas purity (vol%)	>99.5	>99.999	>99.99
System response	Seconds	Milliseconds	na
Stack lifetime (h)	60k to 100k	20–60k	na
Technology status	Mature	Commercial	R&D

membrane water electrolysis" in the title yielded only 20 papers (over the period 2012–2019). The concept and chemistry of AEM water electrolysis is shown schematically in Fig. 1 and compared to PEM water electrolysis. Research coordination in this area has been boosted recently by significant US DOE efforts<sup>19</sup> in developing AEM electrolysis and by the EU through its FCH-JU funding programme.<sup>20</sup>

AEM electrolyzers work with an alkaline environment at the membrane interface provided by the immobilized positively charged functional groups on the polymer backbone or on pendant polymeric side chains. While the largest impediments to the development of AEM systems are membrane stability and ionic conductivity, an improved understanding of how to integrate catalysts into AEM systems is necessary. Research on AEM systems to date has been limited to the laboratory scale with focus on developing electrocatalysts, membranes and understanding operational mechanisms with the general objective of obtaining a high efficiency, low cost and stable AEM devices. Table 2 lists the most significant recent literature reports on AEM systems. The most important materials (catalysts, membranes, and ionomers) and conditions (electrolyte, operating temperature) are listed along with the best voltage current performance reported.

**2.3.1 Current intellectual property on AEM electrolysis and commercial AEM system development.** A review of published intellectual property relating to AEM water electrolysis was conducted (20/11/2019 ESPACENET). This review showed 634 documents dealing with anion exchange membranes, ten deal directly with AEM water electrolysis as opposed to 151 that focus on fuel cells. The majority of relevant patents and applications are owned by a variety of universities and companies of which H<sub>2</sub> production by water electrolysis is not a primary occupation. Two companies have recently reported development of AEM electrolysis devices; ACTA (now Enapter)<sup>21</sup> and Proton Onsite.<sup>22,23</sup> Proton Onsite demonstrated an electrolyser stack with a LiCoO<sub>2</sub> anode and a Pt/C cathode (1000 h at 400 mA cm<sup>−2</sup> average cell voltage 2.0 V). The stack was fed with 1% KHCO<sub>3</sub> as water feed. The Enapter data shows 0.47 A cm<sup>−2</sup> (voltage loss

0.1 mV h<sup>−1</sup>) with 1% K<sub>2</sub>CO<sub>3</sub>/KHCO<sub>3</sub> feed at 50 °C and PGM-free catalysts.

### 3. Critical AEM components

In the following sections we describe recent developments in the critical components of AEM electrolysis (PGM free HER and OER catalysts and anion exchange membranes). Auxiliary cell components such as bipolar plates and current collectors are not covered as we believe these aspects lie outside the scope of this review.

#### 3.1 PGM-free electrocatalysts

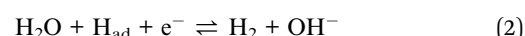
The development of non-noble metal catalysts for both the HER and the OER is crucial to reducing the capital cost of AEM water electrolysis. The challenges lie in optimizing chemical composition, stability and activity of such materials. Because of the relatively low mass specific activity when compared with noble metals, large catalyst loadings are required and this leads to large Ohmic resistance losses.

**3.1.1 HER catalysts.** HER kinetics are well known to be sluggish under alkaline conditions (compared to low pH) especially on PGM-free metals. HER kinetics are two or three orders of magnitude less at high pHs in AEM electrolysis compared to PEM conditions.<sup>24,25</sup>

The HER in alkaline media proceeds by the initial dissociation of water and the formation of hydrogen intermediates (H<sub>ad</sub>) in the Volmer step (eqn (1)):<sup>26</sup>



followed by either the electrochemical Heyrovsky step (eqn (2)):



or the chemical Tafel recombination step (eqn (3)):





Table 2 State of the art literature reports of AEM water electrolysis components and cell conditions

Membrane electrode assembly (MEA) components		Cathode		Ionomer/binder		Cell		Current dens. A cm <sup>-2</sup>		Cell temp. °C		Reference	
Anode	Membrane					Water feed	Voltage (V)	0.399	50	7			
IrO <sub>2</sub>	A-201 Tokuyama	Pt black	AS-4			Deionized water	1.8	0.399	50	7			
CuCoO <sub>3</sub>	A-201 Tokuyama	Ni/CeO <sub>2</sub> -La <sub>2</sub> O <sub>3</sub> /C	PTFE			1% K <sub>2</sub> CO <sub>3</sub> / KHCO <sub>3</sub>	1.9	0.47	50	21			
Pb <sub>2</sub> Ru <sub>2</sub> O <sub>6.5</sub>	Chloromethylated PSF	Pt black	PSF-TMA <sup>+</sup> Cl <sup>-</sup>			Ultrapure water	1.8	0.4	50	22			
Ni-Fe	(xQAPS)	Ni-Mo	(xQAPS)			Ultrapure water	1.85	0.4	70	33			
CuCoO <sub>x</sub>	A-201 Tokuyama	Pt/C	AS-4			K <sub>2</sub> CO <sub>3</sub> 10%	1.95	1	50	113			
IrO <sub>2</sub>	FAA-3-50	Pt/C	FAA-3-Br			1 M KOH	1.9	1.5	70	134			
NiCoO <sub>x</sub> /Fe	FAA-3	Pt black	FAA-3			Pure water	2.25	0.8	50	53			
Ni	A-201 Tokuyama	Ni	—			1 M KOH	1.9	0.15	50	31			
CuCoO <sub>3</sub>	LDPE-g-VBC	Ni/CeO <sub>2</sub> -La <sub>2</sub> O <sub>3</sub> /C	PTFE			1% K <sub>2</sub> CO <sub>3</sub> / KHCO <sub>3</sub>	2.1	0.46	50	143			
Cu <sub>0.7</sub> CO <sub>2.3</sub> O <sub>4</sub>	QPDTB	Nano Ni	Poly(DMAEMA- <i>co</i> -TFEMA- <i>co</i> -BM)			Deionized water	1.9	0.1	50	132			
CuCoO <sub>3</sub>	Mg-Al layered double hydroxide	Ni/CeO <sub>2</sub> -La <sub>2</sub> O <sub>3</sub> /C	PTFE			1% K <sub>2</sub> CO <sub>3</sub> / KHCO <sub>3</sub>	2.2	0.28	70	136			
Ce <sub>0.2</sub> MnFe <sub>1.8</sub> O <sub>4</sub>	FAA-3-PK-130	Pt on Ti	—			Deionized water	1.8	0.3	—	58			
Pd/TNTA web	A-201 Tokuyama	Pt/C	PTFE			2 M NaOH	2	2	80	163			
IrO <sub>2</sub>	Piperidinium-poly(2,6-DPO) LSCPi	Pt/C	5 wt% LSCPi			Deionized water	1.8	0.5	50	90			
CuCoO <sub>x</sub> (on Ni foam)	A-201 Tokuyama, FAA-3,FAA-3-PP-75	Ni/(CeO <sub>2</sub> -La <sub>2</sub> O <sub>3</sub> )/C on carbon paper	I2			1% K <sub>2</sub> CO <sub>3</sub>	1.95	0.5	60	55			
CuCoO <sub>x</sub> (on Ni foam)	A-901 Tokuyama	Ni/(CeO <sub>2</sub> -La <sub>2</sub> O <sub>3</sub> )/C on carbon paper	I2			1% K <sub>2</sub> CO <sub>3</sub>	2.1	0.5	50	54			
NiCo <sub>2</sub> O <sub>4</sub>	Polyethylene based radiation grafted	Pt	Poly(styrene- <i>b</i> -poly(ethylene/butylene)- <i>b</i> -polystyrene			0.1 M KOH	1.65	0.1	60	59			
NiCo <sub>2</sub> O <sub>4</sub> on steel mesh	Homemade, not specified	Powder catalyst, Acta 4030 (PGM free)	Homemade, not specified			DI-water	1.86	0.4	60	60			
Cu <sub>x</sub> Co <sub>3-x</sub> O <sub>4</sub>	PTFE based	Pt/C	q-ammonium polymethacrylate			DI-water	1.6 (2.0)	0.1 (0.4)	22	57			
Cu <sub>x</sub> Co <sub>3-x</sub> O <sub>4</sub>	Developmental AEM with quaternary ammonium functional groups	Pt/C	—			1 M KOH (DI-H <sub>2</sub> O)	1.9 (2.0)	1.4 (0.2)	25	140			
NiFe <sub>2</sub> O <sub>4</sub>	Sustainion 37-50	Nafion	NiFeCo			1 M KOH	1.9	1	60	125			
NiAl	HTM-PMBI	—	NiAlMo			1 M KOH	2.1	2	60	129			

The  $\text{H}_2\text{O}$  dissociation (eqn (1)) is typically a slow reaction and hence it is generally accepted that initial water dissociation is the rate-determining step. Alkaline HER is also more complex than acid HER with  $\text{H}_{\text{ad}}$ , hydroxyl adsorption ( $\text{OH}_{\text{ad}}$ ), and water dissociation all important species/processes to be optimized in developing catalyst materials.<sup>27,28</sup> In a nutshell, the HER in alkaline media requires the breaking of strong covalent H–O bonds (in water) which is a difficult first-up reaction.<sup>29</sup> This section discusses recent advances in the development of PGM-free catalysts for the HER under alkaline conditions. Emphasis will be given to materials tested in complete AEM electrolysis cells.

A large number of Ni-based HER electrocatalysts have been investigated in the literature as potential PGM-free materials. They generally show significantly inferior activity with respect to Pt benchmark catalysts. Commercial Ni nanopowder ( $2 \text{ mg cm}^{-2}$ ) was used in an AEM water electrolyser with a pure water feed and produced  $0.3 \text{ A cm}^{-2}$  at  $1.8 \text{ V}$ .<sup>30</sup> Other researchers used low loading Ni nanoparticles electrodeposited onto carbon paper ( $8.5 \text{ }\mu\text{g cm}^{-2}$ ) as HER catalyst in an AEM electrolyser. With a  $1 \text{ M KOH}$  feed  $0.15 \text{ A cm}^{-2}$  was reached at  $1.9 \text{ V}$  cell potential.<sup>31</sup> The activity and stability of Ni by itself is hence relatively poor. Combination with other transition metals or oxides or as sulphides, selenides, nitrides or phosphides has been used as strategy to obtain improved performance.

Ni supported on a mixed oxide and carbon material ( $\text{CeO}_2\text{--La}_2\text{O}_3/\text{C}$ ) has been employed in an AEM electrolyzer using a mild alkaline electrolyte ( $1\% \text{ K}_2\text{CO}_3/\text{KHCO}_3$ ) operating at pH 10–11.<sup>21</sup> Cathode catalyst loading was shown to have the greatest influence on cell performance. Cathode catalyst loading was varied from  $0.6$  to  $7.4 \text{ mg cm}^{-2}$ , resulting in cell potentials ranging between  $2.01$  and  $1.89 \text{ V}$  at  $470 \text{ mA cm}^{-2}$  ( $T_{\text{cell}} = 50^\circ\text{C}$ ). The measured alternating-current (AC) resistance at  $1 \text{ kHz}$  varied between  $0.218$  and  $0.132 \Omega \text{ cm}^2$  for catalyst loading ranging between  $0.6$  to  $7.4 \text{ mg cm}^{-2}$ . The cell performance parameters were directly related to the cathode catalyst loading with the highest loading producing the best performance despite the thicker electrode layer.

In alkaline media Ni–Mo alloys have been reported to have the best activity of PGM-free catalysts.<sup>32</sup> Zhuang and co-workers first reported an AEM water electrolysis cell working with pure water in 2012 with PGM-free electrocatalysts.<sup>33</sup> A Ni–Mo composite catalyst was employed for the HER.<sup>34</sup> The challenge when removing the electrolyte from the water feed is to have sufficiently high Ni–Mo loading to avoid high Ohmic losses due to the resulting thick electrode. A co-deposition procedure was used to fill a stainless steel skeleton with sufficient Ni–Mo catalyst precursor. Annealing at  $500^\circ\text{C}$  in  $\text{H}_2$  led to the active catalyst that exhibited a very low HER overpotential ( $0.11 \text{ V}$  at  $0.4 \text{ A cm}^{-2}$  in  $1 \text{ M KOH}$ ).<sup>34</sup> Recently, a mixed phased catalyst, composed of crystalline Ni-rich Ni–Mo alloy nanoparticles embedded in a Mo-rich oxide matrix was prepared by Patel and co-workers.<sup>35</sup> This material has low activity toward hydrogen evolution. However, its activity markedly increased upon activation by postdeposition reductive annealing or by including carbon black as a catalyst support. These researchers concluded that the HER activity is limited not only by kinetics but also by

electrical resistivity arising from thin oxide layers at the interfaces between the Ni–Mo alloy nanoparticles. On the other hand, it has been consistently reported that a mix of metallic and oxidic species at the catalyst surface is beneficial for HER/HOR, most probably related to the simultaneous need of adsorption sites for hydroxidic (oxidic) and hydride-type species.<sup>36,37</sup>

Zhang *et al.* prepared a  $\text{MoNi}_4$  electrocatalyst supported on  $\text{MoO}_2$  cuboids on Ni foam ( $\text{MoNi}_4/\text{MoO}_2@\text{Ni}$ ).<sup>39</sup> A reduced energy barrier of the Volmer step, was responsible for the high HER activity under alkaline conditions. The same authors made  $\text{MoNi}_4/\text{MoO}_{3-x}$  nanorod arrays with similarly high activity.<sup>38</sup> Their combined results reveal that this class of alloy exhibits a near zero onset potential, a very small overpotential of  $1 \text{ mV}$  at  $10 \text{ mA cm}^{-2}$ , and a Pt-like Tafel slope of  $30 \text{ mV dec}^{-1}$  in alkaline media, which are comparable to Pt and outperforms all other state-of-the-art Pt-free catalysts reported (Fig. 2). This catalyst was also shown to be stable during short constant current testing (Fig. 2c). The active sites were determined to be metallic  $\text{MoNi}_4$  and oxygen-deficient  $\text{MoO}_{3-x}$ . After an electrochemical scan from  $1.17$  to  $1.72 \text{ V}$ , the catalyst lost HER activity (Fig. 2d) which was associated with irreversible oxidation of  $\text{Mo}^0$ ,  $\text{Mo}^{4+}$  and  $\text{Mo}^{5+}$  to  $\text{Mo}^{6+}$  and  $\text{Ni}^0$  to  $\text{Ni}^{2+}$  species conducting (from XPS).

Poor conductivity of transition metal oxides makes them unsuitable for the HER in general. Some examples however have shown promise; Mo- or W-based oxides are examples. Porous  $\text{MoO}_2$  nanosheets prepared on Ni foam by Jin *et al.* were found to be highly active and stable for the HER in alkaline media.<sup>40</sup> Ni–NiO nanostructures supported on CNTs prepared by Gong and co-workers showed excellent activity ( $100 \text{ mA cm}^{-2}$  at  $100 \text{ mV}$  overpotential).<sup>41</sup> The remarkable performance of this catalyst is likely to be due to a combination of synergistic effects of the nano-interfaces (Ni, NiO and CNT) and the high intrinsic conductivity of the carbon nanotubes. A water electrolyser was

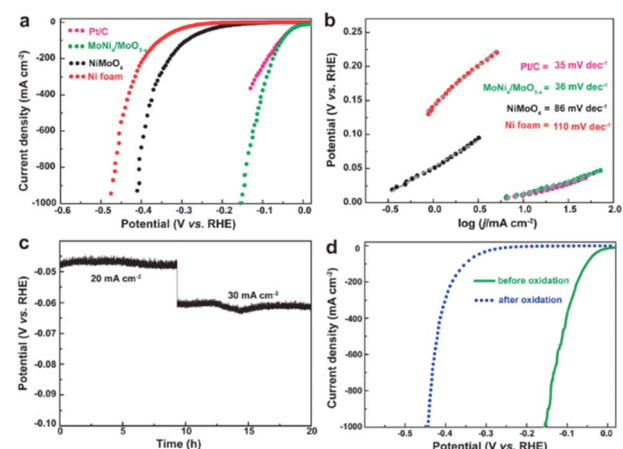


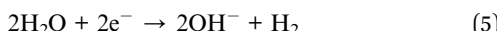
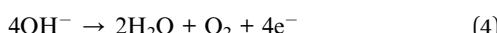
Fig. 2 (a) LSV curves for Pt/C, Ni foam,  $\text{NiMoO}_4$ , and  $\text{MoNi}_4/\text{MoO}_{3-x}$ . (b) The corresponding Tafel plots. (c) Short-term stability test of  $\text{MoNi}_4/\text{MoO}_{3-x}$ . (d) LSV curves of  $\text{MoNi}_4/\text{MoO}_{3-x}$  for HER before and after electrochemical oxidation.<sup>38</sup> Reprinted from ref. 38 with permission from John Wiley and Sons.



tested with this catalyst as cathode and achieved a current density of  $20 \text{ mA cm}^{-2}$  at a cell voltage of 1.5 V in 1 M KOH (membrane-less).

In summary, there are very few reports of PGM-free HER catalysts applied in complete AEM electrolyzers. These are simple Ni-based or Ni-supported on mixed oxide-carbon supports. By comparison, there are many studies of HER catalysts with only half-cell electrochemical characterization. Of all of these, quite remarkable activity, approaching that of Pt, has been demonstrated with Ni-Mo alloyed materials making this class of HER catalyst the most promising for application in AEM electrolyser cells. Engineering rather than chemical solutions may be required to exploit successfully these materials in AEM electrolysis cells on a larger scale.

**3.1.2 OER catalysts.** For the oxygen evolution reaction (OER) under alkaline conditions the half-cell reaction involves the consumption of  $\text{OH}^-$  anions which have to be transported through the anion exchange membrane after formation at the cathode where water is consumed (eqn (4) and (5)).



The OER requires the transfer of four electrons per  $\text{O}_2$  molecule whereas for the HER reaction only two electrons need to be transferred for the formation of a single  $\text{H}_2$  molecule. This gives rise to inherent sluggish OER kinetics, a significant contribution to the cell voltage and in many cases to a more complex mechanism as four  $\text{OH}^-$  ions need to take part in the catalytic cycle. When the water feed contains an electrolyte such as KOH this aids the reaction by supplying  $\text{OH}^-$  to the active sites. In the case of AEM technology the only source of  $\text{OH}^-$  is the ion conducting ionomer.

Regarding the OER mechanism, many models have been proposed recently. For the active and alkaline stable (oxy) hydroxides of the 3d-transition metals such as Mn, Fe, Co, and Ni it is consensus that  $\mu$ -oxo-bridged  $\text{MO}_6$ -units play an important role to facilitate the  $\text{OH}^-$  bonding, further oxidation and release of molecular  $\text{O}_2$ .<sup>42,43</sup>

Excluding the vast amount of work which has been conducted in concentrated KOH the following catalysts are described as effective OER catalysts in dilute KOH,  $\text{K}_2\text{CO}_3$ /KHCO<sub>3</sub> or deionized water (see also Table 2). Another important review has been collected by the Bessarabov group.<sup>44</sup>

**3.1.2.1 Ni-based OER catalysts.** Recent research has shown that Ni-Fe catalysts offer improved activity with respect to pure Ni catalysts.<sup>45</sup> The best result using deionized water reported to date is still the fundamental work of Xiao *et al.* from 2012 with a Ni-Fe anode (xQAPS membrane, Ni-Mo cathode, 70 °C and pure water feed) produced by solid-state electrochemical reduction reaching a current density of  $0.6 \text{ A cm}^{-2}$  at 1.9 V cell voltage (Fig. 3).<sup>33</sup> In addition to the ionomer used a PTFE binder was used for electrode preparation based on a Ni foam. On the other hand after running at  $0.4 \text{ A cm}^{-2}$  for eight hours a degradation of 50 mV was already observed. The authors suspect that the NiFe-anode might cause degradation as iron

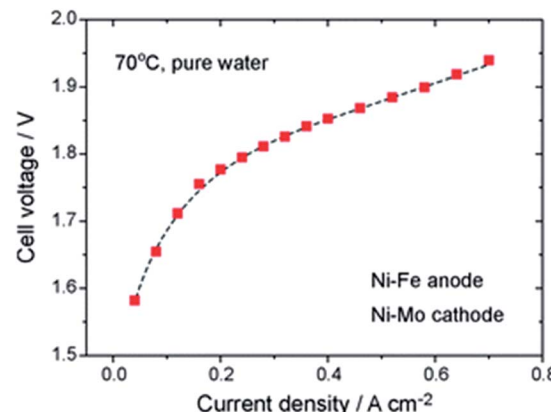


Fig. 3 Cell performance of the first prototype of an AEM water electrolysis system using Ni-Fe anode and Ni-Mo cathode and working only with pure water.<sup>33</sup> Reproduced from ref. 33 with permission. Copyright @ 2014. Royal Society of Chemistry.

leaching can occur at the anode and be redeposited at the cathode.<sup>46</sup> As such this system of catalysts worked equally well as it has been reported with Ir (anode) and Pt (cathode) for example by Leng *et al.* (also using deionized water, Tokuyama membrane A-201).<sup>47</sup> The Fe is useful in order to enhance the catalytic activity towards  $\text{O}_2$  evolution and the mechanistic details and active species are heavily discussed in recent years.<sup>48–51</sup> Indeed, simple physical mixing of  $\text{Ni}(\text{OH})_2$  and  $\text{Fe}(\text{OOH})$  leads to atomically intermixed Ni-Fe catalysts with unexpectedly high OER activity.<sup>52</sup> Xu and co-workers investigated  $\text{NiCoO}_x$ -based catalysts in AEM electrolysis and found excellent performance that was further improved by adding Fe species to the particle surface.<sup>53</sup>

**3.1.2.2 Other PGM-free-based OER catalysts.** The  $\text{Cu}_x\text{Co}_{3-x}\text{O}_3$  spinel anode catalysts described by Vincent *et al.* and several times by Wu and Roggan were shown to have optimized performance in combination with a  $\text{Ni}/(\text{CeO}_2\text{-La}_2\text{O}_3)/\text{C}$ ,  $30 \text{ mg cm}^{-2}$ , cathode (often tested in combination with Pt) and most stable with the A201-Tokuyama membrane, but were also tested with FAA-3 membranes (Table 2).<sup>54–57</sup> They used the I2 Acta Spa ionomer and tested the MEA for 200 hours in a  $5 \text{ cm}^2$  cell. Although performing quite well with PGM-free catalysts, the degradation rate was significant with an average voltage increase of  $2.37 \text{ mV h}^{-1}$ . With the same type of OER catalyst Pavel *et al.*<sup>21</sup> obtained similar performance in 2014. In this case the degradation in the cell test was estimated to be close to  $0.2 \text{ mV h}^{-1}$  (approximately 200 mV in a 1000 h cell test). An interesting class of OER catalyst based upon Ce incorporation into  $\text{MnFe}_2\text{O}_4$  crystal lattice provided improved activity and conductivity.<sup>58</sup> At 25 °C, the single cell with  $\text{Ce}_{0.2}\text{MnFe}_{1.8}\text{O}_4$  exhibited a current density of  $300 \text{ mA cm}^{-2}$  at 1.8 V. Notably,  $\text{Ce}_{0.2}\text{MnFe}_{1.8}\text{O}_4$  demonstrates a durability of >100 hours in continuous electrolysis.

The Bessarabov group using the  $\text{Cu}_x\text{Co}_{1-x}\text{O}_3$  anode and a very thin (9  $\mu\text{m}$  thick) A209 membrane showed stable performance for almost 200 h at *ca.* 2.1 V cell voltage at a current density of  $500 \text{ mA cm}^{-2}$  with a degradation rate of  $0.2 \text{ mV h}^{-1}$ .<sup>54</sup>



Gupta *et al.* were investigating the  $\text{NiCo}_2\text{O}_4$  catalyst as an anode at 60 °C in 0.1 M KOH (Pt cathode) with a reasonable performance of 100 mA cm<sup>-2</sup> with a polyethylene based radiation grafted AEM and a polystyrene-based ionomer.<sup>59</sup> Unfortunately, no tests in deionized water are shown and degradation studies on the long term have not been put forward.

In conclusion, the number of PGM-free catalysts used as anodes in AEM electrolysis with a deionized water feed is small. The very active Ni-Fe catalysts (layered double hydroxides or oxyhydroxides) as well as the Ni- and Cu/Co-mixed spinel-type oxides remain the most likely candidates for an efficient anode in AEM water electrolysis. The only publications focusing on a combination of deionized water and PGM-free catalyst materials in AEM electrolysis that obtained reasonable activity originate from the year 2012 (ref. 33) and 2018.<sup>60</sup> It is clear that fast development of preparation methods and rational catalyst design principles together with the necessity to substitute Ir-based and Pt precious metal catalysts will drive AEM electrolysis.

A further challenge remains the preparation of solid polymer electrolyte membranes with fast  $\text{OH}^-$  transport and low degradation at high temperatures. Additionally, the challenge remains to optimize the catalyst loadings and the catalyst/ionomer ratio in order to maximize the cell performance and the ionic contact between electrodes and anion exchange membrane.<sup>61</sup> These aspects will be discussed in the following sections.

## 4. Anion exchange membranes and ionomers

Anion exchange membranes and ionomers are the fundamental core components of AEM electrolysis technology. Generally, they are formed by a polymer backbone with anchored cationic groups that confer anion selectivity.<sup>62</sup> Most often, the anion exchange group consists of trialkyl quaternary ammonium salts attached to polymeric backbones like polystyrene, polysulfone, poly(ether sulfone) or poly(phenylene oxide) by benzylic methylene groups (see for example<sup>63</sup> and references cited within).

The major shortcoming of anion exchange materials is their limited thermal stability, especially at high pH.<sup>64</sup> Two main mechanisms, namely Hofmann elimination and nucleophilic attack of hydroxide on N-alkyl groups ( $\text{S}_{\text{N}}2$  mechanism) lead to degradation of anion-exchange groups at high temperature under basic conditions.<sup>65</sup> Other degradation mechanisms have also been recently identified such as the electrochemical oxidation of the adsorbed phenyl group (in the polymeric ionomer) on oxygen evolution catalysts.<sup>66</sup>

This limitation has important consequences for the long-term stability of AEM electrolyzer systems as well as the operational temperature limits. Consequently, extensive recent research has involved the development of new anion exchange materials with higher thermal/chemical stability in alkaline medium for the use in electrochemical applications (Fig. 4). Most AEMs have been developed for alkaline fuel cells (AEMFCs) (see reviews by Ran *et al.*,<sup>67</sup> Hagesteijn *et al.*,<sup>68</sup>

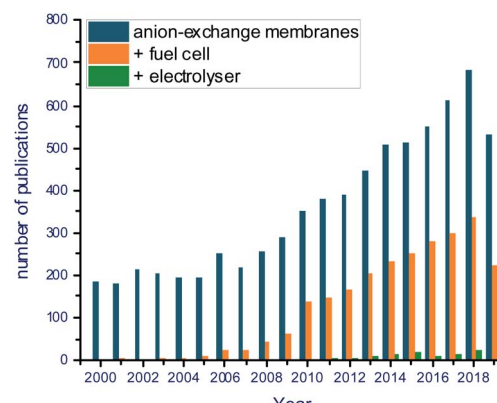


Fig. 4 Development of annual number of publications in the field of anion exchange membranes (from Web of Science (access 18.10.2019)). Search terms in topic: anion AND exchange AND membrane (AND fuel AND cell; AND electrolyser).

Hickner *et al.*,<sup>69</sup> Merle *et al.*,<sup>70</sup> Couture *et al.*,<sup>71</sup> and Wang *et al.*,<sup>72</sup>). The advantages of alkaline AEM-based systems when compared to CEM-based systems in electrochemical applications have been highlighted in review papers by Varcoe *et al.*,<sup>55</sup> Gu *et al.*,<sup>73</sup> and Paidar.<sup>74</sup> Bodner (general alkaline electrolysis) has paid special attention to alkaline electrolysis.<sup>75</sup> However, less attention has been paid to membrane-based alkaline water electrolyzers (see review by Vincent and Bessarabov<sup>44</sup>).

The following section reviews the development of new temperature and alkaline stable AEMs. The last section describes AEMs used specifically in AEM water electrolyzers.

An unexpected high thermal stability in alkaline medium (20% NaOH, 100 °C) has been reported for spirocyclic bis-2-biphenylene ammonium iodide.<sup>76</sup> Since the synthesis of this compound is not straightforward, simpler and easier to synthesize molecules have to be developed mimicking this structure. Marino and Kreuer reported on the thermal stability of quaternary ammonium salt model compounds.<sup>77</sup> The most stable compound in this study was 6-azonia-spiro[5.5]undecane followed by N,N-dimethylpiperidinium salt, the former one having a similar structure to that described by Hellwinkel and Seiffert.<sup>76</sup> A similar study was performed by Gu *et al.*,<sup>78</sup> showing that 5-azoniaspiro[4.5]decane possesses the highest alkaline stability (2 N NaOH 80 °C, 168 h) among the tested compounds. Linear (water soluble) polymers bearing 5-azoniaspiro[4.4]nonane moieties in the backbone, obtained by cyclopolymerisation of N,N-diallylpyrrolidinium chloride showed no degradation after treatment in 2 N NaOH at 80 °C after 168 h.<sup>79</sup> Even additional treatment at 120 °C for 18 h resulted in no decomposition. The Jannasch group at Lund University (Sweden) reported several approaches for the preparation of alkaline stable anion exchange materials based on spirocyclic quaternary ammonium salts.<sup>80-87</sup> These approaches include incorporation of such functional groups into the polymer backbone<sup>80-83</sup> or directly attached to the polymer backbone *via* benzylic methylene groups,<sup>86</sup> as a sidechain with different spacer lengths<sup>85</sup> and different ion exchange groups<sup>87</sup> or as homopolymer in an interpenetrating network with



brominated poly(phenylene oxide) as second component.<sup>84</sup> Direct attachment of spirocyclic ammonium groups (piperidinium) was achieved by reacting tetrakis(bromomethyl)benzene units in poly(ether sulfone) with N-heterocycles of different ring size (5–7).<sup>86</sup> Depending on the ring size, hydroxide conductivities were found to be in the range of 19 to 110 mS cm<sup>-1</sup> (the smaller the ring the higher the conductivity). While the materials were stable in alkaline solution (1 N NaOH) at 20 °C, degradation of the spirocyclic quaternary ammonium group was observed after 7 days at 40 °C by <sup>1</sup>H NMR spectroscopy. Treatment at 60 °C resulted in an additional degradation of the polymer backbone. The same chemistry, namely conversion of tetrakis(bromomethyl)benzene with N-heterocycles (bipiperidine or trimethylenedipiperidine), was used to prepare anion exchange materials with the ion exchange group in the polymer backbone.<sup>83</sup> Both materials showed high stability under alkaline conditions (1 N KOH) at 80 °C (no degradation after 672 h) and slight degradation after 336 h at 120 °C. For the trimethylenedipiperidine-based material, no degradation was observed even after 1896 h storage in 1 M KOH at 80 °C. Since these materials are water soluble, membranes were prepared from blends with poly(benzimidazole) (ionic crosslinking) containing 70–80 mass% of the respective ionomer. Hydroxide conductivities at 90 °C under fully hydrated conditions were in the range from 70 (80 mass% ionomer) to 120 mS cm<sup>-1</sup> (70 mass% ionomer). This result was explained by increasing water uptake with increasing ionomer content in the blend (up to 450%). Another method to obtain anion exchange materials and membranes with six-membered heterocycles in the polymer backbone involves the polymerization of N-methyl-4-piperidone and aryl compounds (biphenyl, *p*-terphenyl) and 1,1,1-trifluoroacetone or 2,2,2-trifluoroacetophenone as comonomer and triflic acid as catalyst.<sup>80–82</sup> Quaternary ammonium groups were obtained by reaction of the pendant piperidine moiety with halogenoalkanes<sup>82</sup> or  $\alpha,\omega$ -bis-halogenoalkanes.<sup>81</sup> The latter reaction results either in spirocyclic or crosslinked products.<sup>80</sup> In all cases, products with high alkaline stabilities at elevated temperatures were obtained. Quaternizing the piperidine moiety with long alkyl chains resulted in a decreasing alkaline stability due to destabilization of the piperidinium ring and thus facilitating the degradation by ring opening elimination. Maximum ion conductivities (OH<sup>-</sup>-form) were in the range of 100 mS cm<sup>-1</sup> at 80 °C under fully hydrated conditions.

In a comparative study Dang and Jannasch investigated the properties of different hetero cycloaliphatic quaternary ammonium groups.<sup>88</sup> These groups were attached to the polymer backbone (PPO) *via* pentyl spacer chains. Cycloaliphatic quaternary ammonium groups based on 5- and 6-membered rings and tetraalkyl ammonium groups linked to the polymer backbone *via* pentyl spacer chains showed no degradation under the applied test conditions (394 h, 90 °C, 1 M NaOH) (Fig. 5). Larger ring size, methyl substituents in *o*-position to the nitrogen, incorporation of hetero atoms into the ring as well as linkage of the ammonium groups *via* methylene spacers resulted in degradation by Hofmann elimination and/or nucleophilic substitution.

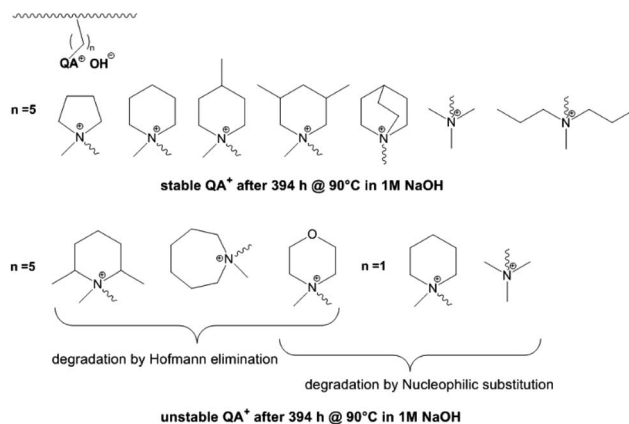


Fig. 5 Stability and degradation mechanisms of different quaternary ammonium groups tethered to a polymer backbone (PPO) by different spacer lengths as revealed by <sup>1</sup>H NMR spectroscopy. Degradation of PPO backbone in these experiments was not detected.<sup>88</sup>

Strasser *et al.* described alkaline stable multiblock copolymers based on polysulfone and diallylpiperidinium hydroxide.<sup>89</sup>  $\alpha,\omega$ -fluorophenylsulfone terminated poly(diallyl piperidinium chloride) was used as macromonomer in the synthesis of polysulfone block copolymers. These block copolymers exhibited a phase-separated morphology as indicated by DSC and AFM measurements. Depending on the IEC (0.90 to 2.02 meq g<sup>-1</sup>) OH<sup>-</sup>-conductivities up to 102 mS cm<sup>-1</sup> were recorded. More importantly, after thermal treatment in methanolic 1 N KOH for 42 days no decomposition of the ion exchange group was observed by <sup>1</sup>H NMR spectroscopy.

Although this class of anion exchange materials has many promising properties with respect to the use in electrochemical processes, only a few papers have been published so far.

Gu *et al.* prepared anion exchange membranes by copolymerization of *N,N*-diallylpyrrolidinium bromide or *N,N*-diallylpiperidinium bromide or *N,N*-diallyl-*N*-hexamethylene iminium bromide, acrylonitrile and styrene.<sup>78</sup> Divinylbenzene (3 mass%) was used as crosslinker. Membranes with a theoretical IEC of 1.2 meq g<sup>-1</sup> (exp. 0.97–1.15 meq g<sup>-1</sup>) were obtained having a hydroxide conductivity in the range of 18.9 to 20.3 mS cm<sup>-1</sup>. As expected from investigations of model compounds in the same study, the highest alkaline stability (168 h, 80 °C, 1 N NaOH) was observed for the membrane based on *N,N*-diallylpiperidinium hydroxide.

Chen *et al.* synthesized a series of anion exchange membranes for alkaline membrane fuel cell applications, based on poly(biphenyl piperidinium) (PBP)/6-azaspido[5.5]undecane functionalized polyphenyl ether (ASU-PPO).<sup>90</sup> The advantages of both polymers were combined by crosslinking. Furthermore, the problem of high water uptake of PBP and the insufficient film-forming property of ASU-PPO were addressed. These crosslinked PBP-ASU-PPO membranes exhibit good ion conductivity (max. 128 mS cm<sup>-1</sup> at 80 °C), durability, and mechanical properties, while the swelling was only 15.7%. The chlorine conductivity decreased only by 13.6% after alkaline treatment in 1 M

NaOH at 80 °C for 2000 h. A maximum power density of 324 mW cm<sup>-2</sup> at current density of 750 mA cm<sup>-2</sup> was recorded in fuel cell tests. Chu *et al.* fixed *N*-methyl-*N*-alkyl-piperidinium moieties to a poly(phenylene oxide) backbone *via* copper catalysed azide alkyn dipolar cycloaddition.<sup>91</sup> Anion exchange membranes prepared by this route exhibited superior alkaline stability over membranes with piperidinium units attached *via* methylene bridges to the polymer backbone (Fig. 5). A conductivity loss of 2% was noted after 560 h at 80 °C in 1 N NaOH. Furthermore, these membranes showed promising performance in fuel cells (H<sub>2</sub>/O<sub>2</sub>) operated at 60 °C (max. power density 116 mW at *ca.* 225 mA cm<sup>-2</sup>; catalyst loading on each electrode was 0.5 mg cm<sup>-2</sup> Pt) and water electrolysis (pure water) at 50 °C (300 mA cm<sup>-2</sup> at 1.8 V) using IrO<sub>2</sub> as anode catalyst and Pt/C as cathode catalyst (loading 1.5 mg cm<sup>-2</sup> each).

Several attempts have been reported using KOH-doped polybenzimidazole membranes in alkaline water electrolysis.<sup>92-95</sup> Diaz *et al.* prepared blend membranes composed of polyvinylalcohol (PVA) and two different polybenzimidazoles, namely PBI (prepared by condensation of isophthalic acid and 3,3',4,4'-tetraaminobiphenyl) and ABPBI (prepared by polycondensation of 3,4-diaminobenzoic acid).<sup>92</sup> The PVA content was varied between *ca.* 10 and *ca.* 33 mass%. The stability of these membranes was improved by crosslinking the PVA with glutaraldehyde (c-PBI, c-ABPBI). Best results in terms of through-plane conductivity at 90 °C were obtained with membranes with a PBI or ABPBI : PVA ratio of 4 : 1 after doping with 15 mass% KOH (PBI and ABPBI: 75 mS cm<sup>-1</sup>; c-PBI: <1 mS cm<sup>-1</sup>, c-ABPBI: 55 mS cm<sup>-1</sup>) or 30 mass% KOH (c-ABPBI: 90 mS cm<sup>-1</sup>). Short-term electrolysis using a c-ABPBI with 20 mass% PVA membrane doped with 15 mass% KOH showed good performance at 70 °C (360 mA cm<sup>-2</sup>) using Ni foam electrodes and 15 mass% KOH solution as feed. In another publication Diaz *et al.* prepared anion exchange membranes using ABPBI and 3-phenyl-6-methyl-3,4-dihydro-2H-1,3-benzoxazin as crosslinker.<sup>93</sup> The membranes were doped by soaking in KOH solutions with a concentration ranging from 1.9 to 4.2 mol L<sup>-1</sup>. While non-crosslinked membranes were brittle after doping with 4.2 mol L<sup>-1</sup> KOH, the crosslinked samples remained stable. The crosslinked membrane, doped with 4.2 mol L<sup>-1</sup> KOH showed an ion-conductivity of 25 mS cm<sup>-1</sup> at room temperature. A current density of 335 mA cm<sup>-2</sup> was attained with a crosslinked membrane doped with 3 mol L<sup>-1</sup> KOH at 70 °C and an applied constant voltage of 2 V. These tests were run in a zero-gap configuration using Ni foam electrodes and 3 mol L<sup>-1</sup> KOH solution as feed. Marinkas *et al.* prepared anion exchange membranes by reacting brominated poly(phenylene oxide) (PPO) with 2-mesitylbenzimidazole.<sup>94</sup> Only materials with an IEC of 1.9 meq g<sup>-1</sup> yielded flexible and self-supporting membranes. An initial conductivity of 8 mS cm<sup>-1</sup> at room temperature was detected. However, these membranes were only stable in 0.5 M KOH at 80 °C. In 1 M KOH a 70% loss in conductivity after 14 days and 30–40% mass loss after 21 days were observed. Water electrolysis experiments were carried out with 3 mg cm<sup>-2</sup> IrO<sub>2</sub> on Ti paper and 1.5 mg cm<sup>-2</sup> Pt/C on carbon paper as cathode and anode catalysts, respectively. In

both cases, PTFE was used as binder material. Furthermore, the anode was fed with 0.5 M KOH, while the cathode was kept dry. Current densities of 85 mA cm<sup>-2</sup> at 1.55 V and 318 mA cm<sup>-2</sup> at 1.8 V were achieved at 50 °C. By comparison, a commercial anion exchange membrane (fumatech FAA-3-PK-75) operated under the same conditions produced 86 mA cm<sup>-2</sup> at 1.55 V and 524 mA cm<sup>-2</sup> at 1.8 V. Differences were explained by the lower water diffusion through the PPO membrane. Blend membranes from mPBI and fumatech FAA-3 with a mPBI content ranging from 67 to 100 mass% (PF21, PF31, PF41, PF51, PBI), where the number denotes the PBI : FAA-3 ratio, were reported.<sup>95</sup> Doping was carried out by immersion in 10 to 30 mass% KOH solutions. The PF41 membrane turned out to be most stable regarding mechanical properties. However, the highest ion conductivity of 166 mS cm<sup>-1</sup> (RT) was observed for the PF51 membrane doped with 25 mass% KOH solution (measurements were carried out in doping solution). Electrolysis experiments were run for example with the PF41 membranes at 60 °C employing different KOH concentrations (10, 15 and 20 mass%) in the supporting electrolyte solution. Ni foam was used as electrode material and catalyst. The polarization performance increased with increasing KOH concentration from ~75 mA cm<sup>-2</sup> at 2 V (10 mass% KOH) to ~175 mA cm<sup>-2</sup> at 2 V (20 mass% KOH). After cell operation at 200 mA cm<sup>-2</sup> for 4 days, a slight increase in current density at 2 V to ~200 mA cm<sup>-2</sup> was detected. Running the electrolysis test with an open cathode resulted initially in a high current density of more than 470 mA cm<sup>-2</sup> at 1.8 V. However, the current density dropped to 230 mA cm<sup>-2</sup> due to leakage of anode electrolyte solution.

A completely different approach to prepare anion exchange membranes was described by Hnát *et al.*<sup>96</sup> Here, a commercially available anion exchange resin (Dowex Marathon A; particle size 10–30 µm; IEC 3.9 meq g<sup>-1</sup>) was incorporated into a LDPE matrix by melt mixing. Membranes with a thickness of 300 µm were obtained by press-molding at 140 °C. These membranes were used to study the impact of liquid electrolyte solution composition on the performance in electrolyzers. Trimethyl ammonium functionalized PPO was used as catalyst binder. The catalysts themselves were NiCo<sub>2</sub>O<sub>4</sub> (2.5 mg cm<sup>-2</sup>) for anode and Pt/C (0.3 mg cm<sup>-2</sup>) for the cathode, each supported on a Ni foam electrode. For long-term electrolysis tests the anode catalyst loading was increased to 8 mg cm<sup>-2</sup> of NiCo<sub>2</sub>O<sub>4</sub>. As expected, membranes in the OH<sup>-</sup>-form showed much higher ion conductivities at 70 °C (67 mS cm<sup>-1</sup>) than membranes in the CO<sub>3</sub><sup>2-</sup>-form (24 mS cm<sup>-1</sup>) or HCO<sub>3</sub><sup>-</sup>-form (18 mS cm<sup>-1</sup>). These differences in conductivity are also reflected in the load curves of alkaline water electrolysis, recorded at 70 °C. At an applied voltage of 1.75 V (85% efficiency) a current density of 266 mA cm<sup>-2</sup> was achieved for the membrane in the OH<sup>-</sup>-form (1 M KOH), while that of the membranes in the CO<sub>3</sub><sup>2-</sup>-form and HCO<sub>3</sub><sup>-</sup>-form was 25 mA cm<sup>-2</sup> and 36 mA cm<sup>-2</sup>, respectively. Long-term tests (100 h) with membranes in OH<sup>-</sup>-form (electrolyte 1 M KOH) and CO<sub>3</sub><sup>2-</sup>-form (electrolyte 0.5 M Na<sub>2</sub>CO<sub>3</sub>) were conducted at 70 °C and a current density of 300 mA cm<sup>-2</sup>. A third experiment was carried out at 50 °C and 300 mA cm<sup>-2</sup> using a 1.95 M KOH. The initial voltages were 1.7 V (KOH, 70 °C), 1.8 V (KOH, 50 °C) and 1.97 V (Na<sub>2</sub>CO<sub>3</sub>, 70 °C). During the



experiments at 70 °C, an increase of cell voltage of 0.4 mV h<sup>-1</sup> (after an initial period of 40 h) and 0.6 mV h<sup>-1</sup> was observed using KOH and Na<sub>2</sub>CO<sub>3</sub>, respectively. It should be further noted that in the case of KOH as electrolyte at 70 °C, the slope of voltage increase could be divided into two regions. The voltage increase at 50 °C was only 0.2 mV h<sup>-1</sup>. Membranes used at 70 °C in the electrolysis experiment showed both a decrease in IEC from 2.45 meq g<sup>-1</sup> to 2.31 meq cm<sup>-1</sup> (KOH) and 2.29 meq g<sup>-1</sup> (Na<sub>2</sub>CO<sub>3</sub>), meaning that both membranes degraded to a certain extend at the applied temperature over 100 h. In contrast, the IEC barely changed for the samples under operation at 50 °C.

In another publication Hnát *et al.* described the preparation of anion exchange materials by conversion of chloromethylated polystyrene-*block*-poly(ethylene-ran-butylene)-*block*-polystyrene (SEBS) with 1,4-diazabicyclo[2.2.2]octane.<sup>97</sup> This material was used as membrane and catalyst binder. Stability tests conducted at 30, 50 and 60 °C in 10 mass% KOH for one week showed no change in conductivity and IEC at 30 °C and a slight decrease by *ca.* 10% at 50 °C. Further increase of temperature to 60 °C resulted in a loss of IEC from 0.76 meq cm<sup>-1</sup> to 0.4 meq cm<sup>-1</sup> and the conductivity dropped from 75 mS cm<sup>-1</sup> to 40 mS cm<sup>-1</sup>. Catalyst coated electrodes were prepared by spraying a catalyst ink, containing the binder in the chloromethylated form and the catalyst (NiCo<sub>2</sub>O<sub>4</sub> (anode); NiFe<sub>2</sub>O<sub>4</sub> (cathode)), onto the nickel foam electrode. After drying, the binder was converted into the anion exchange form by immersing the electrode in ethanolic DABCO solution. The binder and catalyst loadings were 1.11 mg cm<sup>-2</sup> and 10 mg cm<sup>-2</sup>, respectively. Load curves of alkaline water electrolysis were recorded with KOH concentrations ranging from 1 to 15 mass% at 40 °C. The current density at 2 V increased from 70 mA cm<sup>-2</sup> (1 wt% KOH) to 150 mA cm<sup>-2</sup> (15 mass% KOH). Long-term electrolysis tests was performed with bare Ni foam electrodes at 50 °C under galvanostatic conditions at 300 mA cm<sup>-2</sup> using a 10 mass% KOH solution as electrolyte. The dynamic nature of the electrolysis process resulted in a slightly fluctuating voltage around 2.27 V over a period of 150 h. An increase in voltage by 0.02 mV h<sup>-1</sup> was observed during this test, mainly caused by degradation of the membrane. The IEC dropped from initially 0.76 meq cm<sup>-1</sup> to 0.72 meq cm<sup>-1</sup>, which is comparable to results (0.72 meq cm<sup>-1</sup> after 168 h) obtained from *ex situ* test performed under similar conditions. Žitka *et al.* quaternized SEBS with trimethylamine.<sup>98</sup> This material with an IEC of 0.75 meq g<sup>-1</sup> was used as membrane binder for the catalyst. SAXS measurements indicated a clear phase separation and a lamellar morphology with long periods in the range of 32–35 nm. Since the ion exchange groups are located in the polystyrene microdomains, a very high IEC of 2.7 meq cm<sup>-1</sup> inside these domains and therefore in the ion conducting pathways were estimated from SAXS measurements and degree of functionalization. This high local IEC gives rise to high ion conductivities, which are in the range from 56 mS cm<sup>-1</sup> to 79 mS cm<sup>-1</sup> for 30 to 70 °C. MEAs were prepared with 8 mg cm<sup>-2</sup> NiCo<sub>2</sub>O<sub>4</sub> (anode) and different amounts of binder material ranging from 0.42 mg cm<sup>-2</sup> to 2.67 mg cm<sup>-2</sup>. These were compared with MEAs prepared with a PTFE binder (2.67 mg cm<sup>-2</sup>) and bare Ni foam. The cathode catalyst consisted always

of 0.3 mg cm<sup>-2</sup> Pt and 0.05 mg cm<sup>-2</sup> PTFE as binder. Although not perfect, highest current density (280 mA cm<sup>-1</sup>) at 70 °C and 1.74 V were obtained with 0.42 mg cm<sup>-2</sup> quaternized SEBS as binder and 15 mass% KOH solution as electrolyte. Even with 1 mass% KOH electrolyte solution, membranes in combination with optimized MEA composition delivered comparable performance to industrial water electrolyzers (120–320 mA cm<sup>-2</sup> at 1.8–2 V). In a long-term electrolyser test at 50 °C and 10 mass% KOH, the investigated MEAs showed stable performance (300 mA cm<sup>-2</sup>; 1.78 V) over 800 h.

In summary, the search for stable anion exchange polymeric membranes for water electrolysis is dominated by the screening of the cationic ion selective groups. Enhanced stability has been shown for certain materials. The combination with catalysts materials to form MEAs for testing in cells is the subject of the next section of this review paper.

## 5. Membrane electrode assembly preparation approaches

Traditionally, in alkaline water electrolysis large scale electrodes are based typically on Ni at the anode side<sup>95,99–104</sup> and on Ni or stainless steel on the cathode side of the cell.<sup>105</sup> Various strategies have been employed to improve the efficiency of the electrolysis cell. Such as by increasing the electrode surface area, typically by using RANEY® Ni, or by applying suitable nanostructured electrocatalysts. Two principal approaches have been developed to prepare MEAs:

1. Catalyst-coated substrate (CCS).
2. Catalyst-coated membrane (CCM).

Both techniques will be discussed here, although more attention will be paid to the CCM approach as it offers several advantages over the CCS one. Once all MEA components have been prepared, the MEA is typically assembled by pressing them together directly in the cell hardware. The hot-press approach commonly used with PEM systems is not a suitable option because the metal-based electrode substrates (*e.g.* metal foams) are used, which under such conditions damage the membrane.

Other critical components of the AEM cell like current feeders or bipolar plates are also important in determining overall system cost. The alkaline environment offers the advantage of the broader variety of less expensive materials for these components compared to PEM systems. In PEM water electrolysis, Ti or platinized Ti is the common choice.<sup>106</sup> In alkaline water electrolysis cheaper materials like stainless steel,<sup>107,108</sup> nickel<sup>109,110</sup> or graphite<sup>111,112</sup> have been employed. Despite this potential advantage many studies of AEM systems still utilize Ti materials even if working in alkaline media.<sup>113–115</sup>

### 5.1 Catalyst-coated substrate

The CCS approach benefits from robustness and stability of the catalyst layer.<sup>116</sup> CCS is based on the deposition of the catalyst layer onto the surface of an appropriate substrate. The role of the substrate is to enable electron transfer, support the catalyst layer mechanically and to allow the efficient removal of gaseous



products. Several different materials can be used as the substrate. For the anode side Ti paper,<sup>113,117-119</sup> platinized Ti plates,<sup>120</sup> stainless steel felt,<sup>91</sup> Ni foam<sup>54,55,108,109,115,121,122</sup> or even carbon cloth<sup>123</sup> or carbon paper<sup>22,111,112,124</sup> are reported as substrate materials. Ni is the standard material for alkaline water electrolysis while Ti is generally used for PEM water electrolysis. Nevertheless, both of these materials show high thermodynamic stability as anode support in alkaline water electrolysis. In alkaline environment, stainless steel generally passivates at anodic potentials, which ensures stability. At the same time, however, the passive layer reduces the electrical conductivity of the interface between the electrode and electrolyte. The long-term use of carbon materials as anode substrate can be ruled out due to instability under OER conditions. From a thermodynamic point of view, the stability of carbon under alkaline conditions is up to 18-folds lower than in the acidic environment,<sup>125</sup> (see Pourbaix diagram) due to the fact that  $\text{HO}^-$  ions are excellent nucleophiles, which accelerate carbon degradation.<sup>57</sup> Indeed, carbon is used as fuel at the anode for molten NaOH carbon air batteries.<sup>57</sup>

On the cathode side carbon can be readily used,<sup>54,55,111,113,119,120,122,124,126</sup> as well as Ni<sup>95,101,102,108,115,121,127,128</sup> and Ti.<sup>117,118</sup> The electrode preparation method is predominantly based on spraying a catalyst ink over the activated support surface.<sup>22,54,55,119,120,122,129</sup> Other frequently used techniques include electrodeposition,<sup>109,111,112,121</sup> magnetron sputtering,<sup>124</sup> chemical electroless plating<sup>109,115</sup> and screen printing.<sup>54,55,123</sup> Plasma sprayed electrodes containing non PGMs (NiAl anode and NiAlMo cathode) have been prepared on stainless steel gradient porous metal frameworks.<sup>130</sup> Combined with a HTM-PMBI membrane in an AEM electrolyzer fed with 1 M KOH this CCS approach produced  $2 \text{ A cm}^{-2}$  at 2.1 V (60 °C).

## 5.2 Catalyst-coated membrane

The CCM approach is based on depositing the catalyst directly onto the membrane surface. Hence, the main advantage is the resulting intimate contact of the catalyst with the polymer electrolyte membrane and thus improved ionic conductivity. This also enables a decrease in the catalyst loading<sup>131</sup> while maintaining performance of the MEA. On the other hand, the electrical contact between the current collectors is worse. However, as the electron conductivity of the system is significantly higher than the ionic conductivity of the electrolyte, this seems to be a reasonable trade off. The main obstacle to a wide spread application of the CCM approach lies in the absence of suitable polymeric binder. Only recent advances in alkaline polymer electrolyte research has resulted in increasing interest in this approach.

The most commonly applied method of CCM-MEA preparation is spray coating of a catalyst ink onto the surface of the polymer anion-selective membrane.<sup>131-136</sup> Recently, Ito *et al.* compared the performance of CCM-MEAs prepared by spraying and doctor blade method. Better results were achieved using the spraying technique.<sup>116</sup> The reason is lower resistivity of the cell prepared by this technique. Spraying also allowed easier and more precise control of the catalyst and binder loading.<sup>116</sup> The

decal method, which is commonly used in PEM water electrolysis or fuel cell technologies<sup>137</sup> is not suitable for anion-selective polymer membranes. It is because of the hot-pressing step it includes. Anion-selective polymer membranes suffer from chemical instability when exposed to elevated temperatures,<sup>135,138</sup> which precludes catalyst transfer under high temperature conditions.

Amongst the first papers dealing with the issue of the CCM-MEA for alkaline systems are reports by Wu and Scott.<sup>57,107,133,134,139</sup> These works do not directly focus on the issue of the CCM-MEA preparation and characterisation. They are aimed more at the catalyst or membrane/polymer binder itself using the CCM-MEA based MEAs as an experimental testing technique. Using the radiation grafted anion exchange membrane the best achieved performance reached  $980 \text{ mA cm}^{-2}$  in 1 mol dm<sup>-3</sup> KOH at 25 °C and cell voltage of 1.8 V.<sup>56</sup> However, this MEA showed a degradation rate of 22.3 mV hour<sup>-1</sup> (during 11 hours of the chronoamperometry experiment at 300 mA cm<sup>-2</sup>, at 30 °C, in deionized water).<sup>134</sup> Three reasons were addressed by the authors to be responsible for the degradation: (i) drying of the membrane due to bubble evolution, (ii) corrosion of the anode components at cell voltages above 2 V and (iii) degradation of the ionomer in the membrane or binder.<sup>134</sup>

Simultaneously, Leng *et al.* published in 2012 work using commercial materials (Tokuyama A201 membrane and Tokuyama AS-4 polymer binder).<sup>132</sup> The CCM-MEA prepared showed, however, only limited stability under the conditions of alkaline water electrolysis. After 27 h of operation at 200 mA cm<sup>-2</sup> in deionized water (50 °C) feed into the cathode compartment only, the cell voltage together with resistivity of the cell increased sharply.<sup>132</sup> The authors however observed recovery of the cell voltage to the initial value when the 1 mol dm<sup>-3</sup> KOH was supplied to the anode chamber. Based on this, the authors concluded that degradation of CCM-MEA was mainly due to the degradation of the ionomer and/or membrane-electrode interface.<sup>132</sup>

Limited stability of the Tokuyama AS-4 polymer binder was recently observed also by Ito *et al.*<sup>116</sup> who, due to the limited stability of the AS-4 polymer binder, prepared mixed MEAs utilizing the CCM approach for the cathode side and the CCS approach for the anode side. The CCS approach allows to use inert poly(tetrafluoroethylene) (PTFE) as binder of the catalyst layer. Ito *et al.* focused primarily on CCM-based MEAs utilizing PGM-free based catalysts.<sup>116</sup> Subsequently, if the PGM-free cathode catalyst ( $\text{CeO}_2\text{-La}_2\text{O}_3$ ) was replaced by Pt (1.7 mg Pt cm<sup>-2</sup>) the performance of the AWE increased from  $40 \text{ mA cm}^{-2}$  to  $300 \text{ mA cm}^{-2}$  at 1.8 V cell voltage.<sup>114,116</sup>

Direct comparison of the CCS and CCM approaches was provided by Park *et al.*<sup>135</sup> Better performance was in this case achieved using CCM approach ( $500 \text{ mA cm}^{-2}$  at 1.8 V) when compare to CCS approach ( $210 \text{ mA cm}^{-2}$  under identical conditions). The explanation given by the authors was due to negative effects of the CCS preparation method on the structure of the catalyst layer increasing mass transport losses demonstrated by electrochemical impedance spectroscopy analysis of the system.<sup>135</sup> On the other hand, Gupta *et al.*<sup>59</sup> observed the



opposite result when the CCM achieved  $200 \text{ mA cm}^{-2}$  at 1.8 V when compared to  $390 \text{ mA cm}^{-2}$  for CCS approach under the same conditions.<sup>59</sup> However, the results not adequately discussed by the authors and the reasons for this observation were not provided.

Comparison of CCS and CCM methods for MEA preparation is not straightforward. It is mainly due to the absence of standard testing protocols. Fig. 6 summarises the data obtained from the literature. Box plot showing the 25<sup>th</sup> and 75<sup>th</sup> percentile, median, average, error bars (showing 10<sup>th</sup> and 90<sup>th</sup> percentile) values and outlying points was chosen to present the data gathered. Obviously, higher performance of AEM water electrolysers are generally achieved, when PGM catalysts<sup>113,117,118,135</sup> and elevated temperatures<sup>109,113,122</sup> are used. Of course, there can be some exceptions *e.g.* work of Wu *et al.*<sup>139</sup> who achieved  $980 \text{ mA cm}^{-2}$  at 1.8 V at 25 °C using Pt as catalyst on cathode and a PGM-free catalyst on anode side of the cell, Liu *et al.*<sup>126</sup> who achieved  $500 \text{ mA cm}^{-2}$  (1.8 V) at 60 °C using PGM-free catalysts or Pavel *et al.*<sup>122</sup> who achieved  $485 \text{ mA cm}^{-2}$  (1.8 V) with no-PGM catalysts at 43 °C. Further, it can be stated that none of the values above 90<sup>th</sup> percentile was measured with pure water as liquid electrolyte. The main conclusion resulting from Fig. 7 is that both CCM and CCS methods of the MEA construction lead in general to similar results.

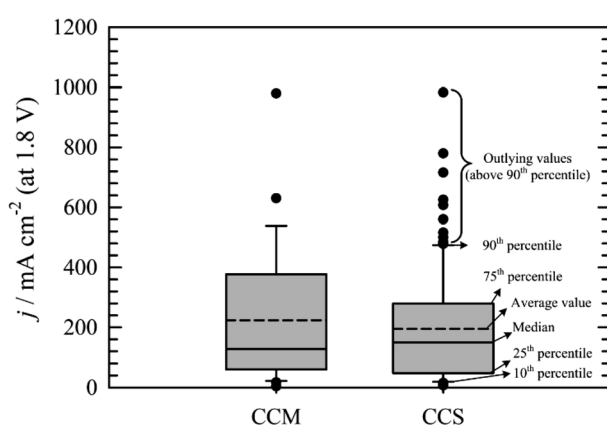


Fig. 6 Comparison of the current densities achieved at cell voltage 1.8 V using the CCM<sup>57,59,106,107,114,116,131–136,139–141</sup> or CCS<sup>22,54,55,95,101–104,108,109,111–113,115,117–124,126–129,142,143</sup> method of MEA construction.

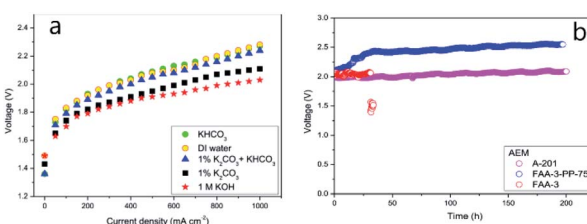


Fig. 7 (a) Polarization curves recorded for different electrolytes and (b) stability of various MEAs: A-201, FAA-3, and FAA-3-PP-75.<sup>55</sup> Reprinted from ref. 55 with permission from Elsevier.

## 6. Influence of the liquid electrolyte on cell performance

Traditionally in alkaline electrolysis a concentrated aqueous KOH solution of up to 30 mass% is circulated through the cell, thus guaranteeing sufficient ionic conductivity to the electrolyte. High cell temperatures are also used which increases electrode kinetics and facilitate separation of the gasses produced from the electrolyte solution. The negative consequences of using such a corrosive electrolyte regard safety issues and poor flexibility. As described above, in order to compete with PEM electrolysis in terms of cost and flexibility, simple demineralised water must be used in AEM. Hence, we will concentrate our discussion on systems that use only pure water or dilute KOH or sodium carbonate/bicarbonate solutions.

### 6.1 Hydroxide solutions

The electrolyte that has been most commonly used in AEM electrolysers are hydroxide solutions (KOH and NaOH). A wide range of concentrations from 0.06 mass% (ref. 114) up to 30 mass% (ref. 127) is reported. This is mainly due to the variation of the types of the materials used as separators. Concentrations above 20 mass% are used in AE together with ion solvating membranes<sup>95,103,104,127</sup> or diaphragm separators.<sup>104,109,128</sup> With anion exchange polymer membranes, concentrations can range from 3 to 10 mass%.<sup>99–101,113,123,126,144</sup> Generally, electrolysis performance improves with increasing concentration of the hydroxide solution.<sup>121,139,145,146</sup> This improvement is explained by the decrease in the polarization resistance of the both electrodes and cell resistance at the same time.<sup>146</sup> While the polarisation resistance decreases linearly with increasing electrolyte concentration,<sup>146</sup> the cell resistance decreases at higher concentrations of the electrolyte less progressively than at the lower ones.<sup>136,146</sup> At low concentrations, the cell resistance can be affected by CO<sub>2</sub> contamination of the KOH solution. (Bi)carbonate ions contaminate the anion selective polymer electrolytes and decrease the ionic conductivity. As the concentration of the KOH solution becomes high enough, a buffer effect decreases the influence of the (bi)carbonates on the conductivity of the membrane and thus the cell resistance remains small.

Only a few studies refer to the utilization of the NaOH as liquid electrolyte.<sup>59,141</sup> NaOH is cheaper than KOH while KOH solutions show much higher values of conductivity<sup>147</sup> when compared to NaOH solutions. More importantly the solubility of K<sub>2</sub>CO<sub>3</sub> is significantly higher than Na<sub>2</sub>CO<sub>3</sub> (ref. 148 and 149) which mitigates the problem precipitate formation and separator scaling. Moreover, KOH solutions are characterised by lower viscosity when compared to NaOH.<sup>150</sup> Thus, KOH provides a more reliable and flexible electrolysis cell operation despite its higher cost.

### 6.2 Bicarbonate/carbonate

Dilute carbonate or bicarbonate solutions have a mildly alkaline pH (10–12) that retains sufficient ionic conductivity.



Additionally, such conditions should provide enhanced stability of cell materials as well as the polymeric AEM/binders.<sup>114,122,143</sup> The ionic conductivity of AEMs is significantly lower in the carbonate or bicarbonate ( $\text{CO}_3^{2-}/\text{HCO}_3^{2-}$ ) form.<sup>151</sup> The electrode reaction kinetics are also lower in carbonate or bicarbonate environment.<sup>151</sup> It has been shown, however, that under high current load the  $\text{OH}^-$  produced at the cathode is transported through the anion selective membrane and exchanges the  $\text{OH}^-/\text{CO}_3^{2-}$  ratio in its bulk. This ratio becomes current dependent.<sup>114,152</sup> Nevertheless,  $\text{CO}_3^{2-}$  ions acting as counter ions are present in certain amount in the membrane even under high current conditions.<sup>114</sup> The membrane resistance thus tends to be always higher than it is in the case of hydroxide liquid solutions. Despite the fact that in the case of the liquid electrolytes utilizing the carbonates or bicarbonates the concentration of  $\text{OH}^-$  ions is lower when compared to hydroxide solutions (pH is lower), the pH value in the bulk of the membrane can generally differ from those of the surrounding solution.<sup>153</sup> Increased number of  $\text{OH}^-$  under higher current load can thus still cause membrane degradation.<sup>151</sup> Most studies use potassium salts, *i.e.*  $\text{K}_2\text{CO}_3$  or  $\text{KHCO}_3$  solutions.<sup>54,55,106,114,116,122,143</sup> These show commonly better performance than with  $\text{Na}_2\text{CO}_3$  or  $\text{NaHCO}_3$ .<sup>141,151</sup> Regardless of the counter-cation ( $\text{Na}^+$  or  $\text{K}^+$ ), when the  $\text{CO}_3^{2-}$  and  $\text{HCO}_3^-$  ions are compared, better results are obtained for  $\text{CO}_3^{2-}$  solutions.<sup>55,122,141,151</sup>

### 6.3 Water

The use of demineralised water is ultimately the most desired solution to make AEM electrolysis a competitive technology. Using pure water as feed, however, brings important new challenges. Ni represents, without any doubts, the standard material for electrode construction in AEM electrolysis. However, under anodic polarisation, it is stable only at pHs >9, ruling out the possibility of using a pure water feed.<sup>154</sup> Ti-based porous materials<sup>115,118,120,132</sup> and/or current collectors<sup>55,141</sup> are suitable but more expensive.<sup>114</sup> Another problem with using deionized water is the influence of  $\text{CO}_2$  on performance. Parrondo *et al.*<sup>22</sup> observed a drop in current density at a cell voltage 1.8 V from  $365 \text{ mA cm}^{-2}$  to  $135 \text{ mA cm}^{-2}$  in just 30 min. This loss was associated with an increase in both high frequency resistance and charge transfer resistance. The authors explained that this phenomenon was due to  $\text{CO}_2$  contamination leading to dissolved carbonate and bicarbonate anions that decrease the ionic conductivity of the membrane and catalytic layer binders.<sup>22</sup> The nature of the AEM ionomer/binder is an important aspect of water fed AEM electrolysis. This material must ensure the mechanical stability of the catalyst layer and at the same time provide ionic conductivity within the catalyst layer. The importance of the AEM binder has been highlighted in the literature. Current density (<15  $\text{mA cm}^{-2}$  at 1.8 V) with no,<sup>115,124,142</sup> or inert binder (*e.g.* PTFE).<sup>114,141</sup> Using PTFE as a binder, Cho *et al.*<sup>118</sup> were able to achieve a current density ( $60 \text{ mA cm}^{-2}$  at 1.8 V) comparable with some of the works utilizing anion selective polymer binders.<sup>107,133,136</sup> However, in the case of the Cho *et al.*, pure water was fed only to the cathode compartment while the anode compartment was fed with 0.5 mol

$\text{dm}^{-3}$  KOH thus ensuring the ionic conductivity within the catalyst layer from the anode side. When an anion exchange polymeric binder is used in the catalyst layer, current densities higher than  $90 \text{ mA cm}^{-2}$  have been obtained.<sup>22,55,57,108,129,134</sup> Obviously, a significant ionic conductivity of the AEM ionomer is required. In some cases poor activity ( $17\text{--}36 \text{ mA cm}^{-2}$ ) was obtained even using ionomers.<sup>135,140</sup> For example Cao *et al.* observed ionic conductivity of their material to be  $1.5 \text{ S m}^{-1}$  at  $25^\circ\text{C}$ ,<sup>140</sup> which is less when compare to papers by Wu *et al.* who used materials with ionic conductivity of  $1.8\text{--}4.0 \text{ S m}^{-1}$  at  $20^\circ\text{C}$ .<sup>57,134</sup>

### 6.4 Comparison of the liquid electrolytes

Performance data of AEM electrolyzers reported in the literature using different electrolytes is summarised in Fig. 9. It clearly shows that using pure water cannot compete with utilization of dissolved ionic electrolytes. The average current density at a cell voltage of 1.8 V with a pure water feed was found to be  $95 \text{ mA cm}^{-2}$ ,  $160 \text{ mA cm}^{-2}$  for (bi)carbonates solutions and  $220 \text{ mA cm}^{-2}$  for KOH solutions (Fig. 9). The best performance reported for water and (bi)carbonate solutions are 450 (ref. 57) and 440 (ref. 122)  $\text{mA cm}^{-2}$  respectively. The best performance of 450  $\text{mA cm}^{-2}$  for circulating water was achieved using CCM based MEA.<sup>57</sup> The high outlying values are generally achieved using PGM catalysts<sup>120</sup> and higher operating temperature.<sup>108</sup> However, in one case at temperature of  $70^\circ\text{C}$  the current density of  $250 \text{ mA cm}^{-2}$  was reached at 1.8 V utilizing PGM-free catalysts.<sup>108</sup> Vincent and co-workers using PGM-free catalysts and commercial membrane/ionomer compared liquid electrolytes.<sup>54,55</sup> With DI water, 1%  $\text{KHCO}_3$ , and 1% ( $\text{K}_2\text{CO}_3 + \text{KHCO}_3$ ) performance was similar (Fig. 7). The voltages at  $400 \text{ mA cm}^{-2}$  were 2.04, 2.03, and 2.0 V, respectively. However, the performances achieved with electrolytes 1%  $\text{K}_2\text{CO}_3$  and 1 M KOH were better than those achieved when using DI water, 1%  $\text{KHCO}_3$ , and 1% ( $\text{K}_2\text{CO}_3 + \text{KHCO}_3$ ).

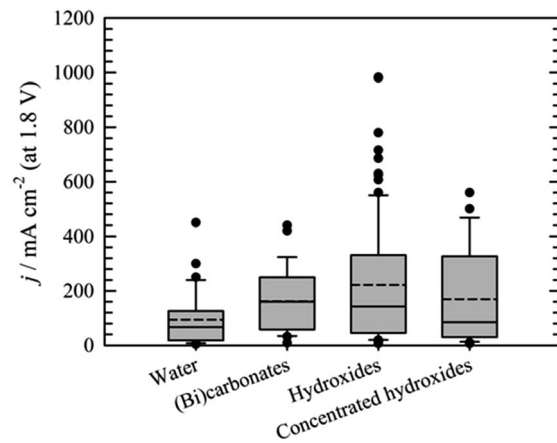


Fig. 8 Comparison of the current densities achieved at cell voltage 1.8 V using water,<sup>22,55,57,107,108,114,115,118,120,124,129,132–136,139–142</sup> (bi)carbonates<sup>54,55,96,106,114,116,122,141,143,151</sup> or hydroxides<sup>55,59,93,95,101–104,109,111–114,117–119,121,123,124,126–128,132,135,136,139,141,145,146,155–159</sup> as liquid electrolyte. Bar for "concentrated hydroxides" represents KOH solutions  $>1 \text{ mol dm}^{-3}$ .



In the case of the (bi)carbonates the best performance was achieved using PGM-free catalyst at 55 °C.<sup>122</sup> Generally, in the case of (bi)carbonate solutions PGM-free catalysts are widely used.<sup>54,55,116,122,141,143</sup> The important parameters found to influence the performance are catalyst load,<sup>122</sup> temperature<sup>54,55,122</sup> and concentration of the solution used.<sup>114</sup>

In the case of the hydroxide solution, situation is slightly different. The reason consists in the fact that hydroxide solutions represent standard test solution and many papers are thus using hydroxide solutions for extreme experiments. Outlying values above percentile 90<sup>th</sup> are thus *e.g.* due to high KOH concentration,<sup>109,121</sup> high operating temperature,<sup>109,113,121</sup> or high operating pressure.<sup>109</sup> Under milder conditions the best performance is commonly achieved utilizing PGMs.<sup>117–119,132,135</sup>

However, as it is possible to see from the last bar in Fig. 8 showing the current densities achieved at a cell voltage of 1.8 V using concentrated KOH solutions (concentrations  $>1 \text{ mol dm}^{-3}$ ), the high concentration of the liquid electrolyte by itself cannot guarantee high current density. The reason in this particular case lies probably in the type of the separator used. Highly concentrated KOH solutions are typically used when diaphragms<sup>102,160</sup> or ion solvating membranes<sup>95,103,104,127</sup> are utilized as the separator of the electrode compartments. In these cases, however, the current densities did not exceed 120 mA cm<sup>-2</sup>.

## 6.5 Arrangement of water or electrolyte circulation in the cell

In AEM electrolysis cells the liquid electrolyte may be circulated through (i) both anode and cathode compartment;<sup>59,126,131,134,161</sup> (ii) anode compartment only<sup>54,55,113,116,117,122,143</sup> and (iii) cathode compartment only.<sup>111,112</sup> A special case involves feeding of both compartments with streams of different composition. Cathode fed with the water and anode with hydroxide or (bi)carbonate solution represents the typical case here.<sup>118,119,132</sup>

In traditional industrial cells the liquid electrolyte flows through both electrode compartments. This is primarily given by utilizing porous diaphragm based separator. In such a case feeding of just one electrode compartment leads to significant electrolyte cross-over. If a dense polymer anion selective membrane is used as a separator, the situation differs. Liquid electrolyte can be fed only to one electrode compartment without significant cross-over. This can result in simplification of the liquid electrolyte circulation and even in simplification of the gas separation and processing due to the possibility to achieve higher purity of the produced gasses.<sup>110</sup> In the literature, electrolyte flowing through both compartments represents the state-of-the-art.<sup>101,103,120,121,126</sup> Leng *et al.*<sup>132</sup> tested different feeding methods in 2012, observing that the best cell stability was achieved with the cathode compartment filled with water and water circulated through the anode side (stable cell voltage for more than 500 h). When water was circulated just through one of the electrode compartments, sharp increase of the cell resistance was observed after 100 h or 250 h of operation for water circulation only through the cathode or anode side respectively. Another direct comparison was recently provided by Park *et al.*<sup>135</sup> Best performance was achieved for the case of

the 1 mol dm<sup>-3</sup> KOH solution circulating through both electrode compartments.

Cathode reaction is connected with H<sub>2</sub> molecule formation under consumption of two H<sub>2</sub>O molecules and release of the two OH<sup>-</sup> ions. If liquid electrolyte is fed to the cathode compartment exclusively, OH<sup>-</sup> ions are transported to the anode compartment across the membrane, accompanied by the solvating shell formed by the water molecules. O<sub>2</sub> evolution at the anode results in producing additional H<sub>2</sub>O molecules. Thus, environment pH in the anode compartment will be close to neutral and thus, it will not satisfy the condition of pH higher than 9 to ensure stability of the Ni-based anode.<sup>110</sup> Therefore, this option does not ensure the corrosion stability of the cell.

Alternatively, the liquid electrolyte can be fed to the anode compartment only. In this case, H<sub>2</sub>, which is generally considered as the main product, can be obtained with higher purity.<sup>110</sup> Such configuration of the cell also allows easier utilisation of the cell as an electrochemical compressor.<sup>143</sup> Nature of the electrode reactions taking place ensures stable pH at both electrodes. Water supply to the cathode, where it is consumed, is ensured through the hydrophilic membrane. Under high current loads, this can be theoretically connected with partial drying out of the membrane. It, in turn, can cause membrane degradation.<sup>162</sup> As it was shown, however, performance of the APEWE with liquid electrolyte fed only to anode compartment showed current density up to 485 mA cm<sup>-2</sup> at cell voltage 1.8 V and stability over 1000 h.<sup>122</sup> Up to 2 A cm<sup>-2</sup> has also been achieved with no water feed to the cathode using Tokuyama A-201 membrane and 2 M NaOH fed to the anode compartment.<sup>163</sup> So, the degradation of the polymer electrolyte membrane seems not to be a critical issue under such conditions.

Literature reveals that circulation of the liquid electrolyte through the both electrode compartments is beneficial from the APEWE performance point of view. However, sufficiently high current densities of about 500 mA cm<sup>-2</sup> at 1.8 V can be reached even with circulation only through anode side.<sup>117,122</sup> Due to the advantages coming from circulation of the liquid electrolyte only through one electrode chamber as discussed earlier the circulation of the liquid electrolyte only through anode side represents the candidate for the future state-of-the-art arrangement.

## 6.6 Long-term stability tests

Comparison of the long-term performance of AEM water electrolyser cells (LTE) published by different authors is difficult. Once again, the reason lies in the absence of standard testing protocols. Some experiments last only for a few hours<sup>120,121,123,124</sup> or tens<sup>103</sup> of hours. The longest experiment was probably performed by Choe *et al.* (more than 2000 hours).<sup>164</sup> However, significant increase of the cell voltage was observed during this experiment due to degradation of the polymer backbone. This is probably due to the type of the polymer backbone used based on poly(arylene ether), which is well known to undergo the chemical degradation (*via* aryl-ether bond cleavage) in alkaline environment.<sup>165–167</sup> This confirms that the choice of suitable



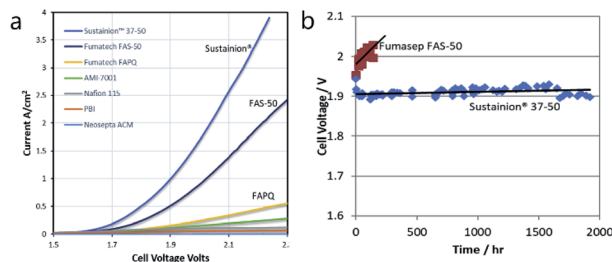


Fig. 9 (a) Comparison of current–voltage response of AEM electrolysis with various membranes in ref. 119. (b) Steady state voltage performance at  $1 \text{ A cm}^{-2}$  with Sustainion 37–50 membrane and FAS-50 membrane ( $60^\circ\text{C}$ , 1 M KOH,  $\text{NiFe}_2\text{O}_4$  anode and  $\text{NiFeCo}$  cathode). Reprinted from ref. 125 with permission from Elsevier.<sup>125</sup>

polymer backbone plays an important role. In this case, however, solution exists and number of polymers stable under alkaline water electrolysis conditions was identified, *e.g.* heteroatom-free all-carbon backbones (like polyolefins or poly-phenylenes).<sup>168</sup> Functional groups, however, are considered more susceptible towards chemical degradation and clear solution does not exists here yet. A constant current experiment showing improved stability (approaching 2000 h) was published by Liu *et al.* (Fig. 9).<sup>125</sup> The Sustainion 37–50 membrane maintained  $1 \text{ A cm}^{-2}$  with PGM-free catalysts ( $60^\circ\text{C}$  and 1 M KOH) although some instability in cell voltage can be noted during the test.

Another interesting feature is, that the  $V$ – $I$  load curves, are usually obtained in the temperature range of 80 to  $90^\circ\text{C}$ ,<sup>55,113,142</sup> while the LTE experiments are typically carried on at temperatures below  $60^\circ\text{C}$ .<sup>122,126</sup> It clearly indicates the poor stability of performance at higher temperatures. It is thus possible to conclude, that short-term performance figures have to be considered carefully, as they often are performed outside the long-term stability conditions window. Interestingly, all of the MEAs tested for more than 400 h were prepared by the CCS approach. The reason consists in the fact, that CCM-MEAs represent significantly more recent approaches to the MEA production and the number of data collected so far is still relatively small. Moreover, as already discussed, the main obstacle in studying this approach consists in the absence of sufficiently stable and conductive polymer electrolytes. In the case of the CCM approach one of the longest experiments lasted for approx. 100 h,<sup>136</sup> which is still is significantly less when compared to the CCS approach. A positive aspect is, that the voltage of the CCM-based MEA in 1 mol  $\text{dm}^{-3}$  KOH at  $50^\circ\text{C}$  and  $400 \text{ mA cm}^{-2}$  was in this case constant, without signs of degradation.<sup>136</sup> Generally, the reasons of CCM-based MEA degradation mentioned in the literature are (i) delamination of the catalyst layer,<sup>132,134,136</sup> (ii) membrane degradation,<sup>134,136</sup> (iii) ionomer degradation,<sup>116,132,134</sup> (iv) drying of the membrane due to gas phase evolution<sup>134</sup> and (v) corrosion of anode components at cell voltage above 2 V.<sup>134</sup> The first three reasons are clearly related to the insufficient stability of the anion selective polymer under conditions of alkaline water electrolysis as discussed above. It is also the reason for slow development in the field of CCM-MEA.

## 6.7 High pressure operation

An important feature of membrane electrolysis is that  $\text{H}_2$  inside the cell can be pressurized. In typical commercial PEM electrolyzers,  $\text{H}_2$  is pressurized to 15–30 bar. Pressurized operation of AEM electrolyzers should be possible as AEMs have similar mechanical properties to PEMs. Ito and co-workers recently investigated the effect of high  $\text{H}_2$  pressure on electrolysis performance up to 8.5 bar.<sup>106</sup> A Tokuyama A201 AEM was used with Pt/C and  $\text{CuCoO}_x$  cathode and anode catalysts respectively. The cell showed pressurized operation (8.5 bar) at the cathode while the anode was operated at atmospheric pressure. Very low crossover of  $\text{H}_2$  to the anode was observed, 0.16 times that of PEM systems as well as low water content in the produced  $\text{H}_2$ . This study confirms that high pressure operation of AEM electrolysis is possible and advantageous.

## 7. Summary

Despite a flurry of recent research activity, AEM electrolysis technology remains at an early stage of development. In this review article we present a panoramic view of the current state of the technology. We have divided the critical components between (i) electrocatalysts for the HER and OER, (ii) membranes and ionomers and (iii) MEA preparation techniques. We have concentrated our review on low-cost materials, in particular, electrocatalysts based upon cheap and abundant metals (PGM-free). Together with these aspects, description of the MEA preparation techniques CCM and CCS are presented. Further, we have reviewed important cell parameters such as temperature, electrolyte composition and flow regime.

### 7.1 Catalysts

Recent reports highlight the problem of the slow kinetics of PGM-free HER catalysts for AEM electrolysis. Low mass activity of Ni-based catalysts leads to high losses from thick catalyst layers in AEM test cells. Nevertheless, very promising candidates based on Ni–Mo alloyed materials have been identified. Electrochemical tests in half cells show HER behaviour similar to Pt benchmark catalysts. Regarding OER, high activity of transition metal mixed oxides has been shown in AEM electrolysis. The best performing materials are  $\text{Cu}_x\text{Co}_{3-x}\text{O}_4$ ,  $\text{NiCo}_2\text{O}_4\text{:Fe}$  and Ni–Fe alloys used in AEM cells on Ni foam supports.

### 7.2 Membranes and ionomers

The chemical stability of AEMs under alkaline conditions has improved markedly due to the development of stabilized functional groups on the polymer backbone. This allows the use of such membranes in AEM electrolysis at higher temperatures for long periods. Less emphasis has been given to the ionomer/binder material used to provide ionic conductivity within the catalyst layer, in part, because of the continued use of liquid electrolytes. Ultimately, a pure water feed will be necessary for AEM electrolysis and the ionomer/binder material will be very important.



### 7.3 MEA preparation and cell performance

The physical and electrochemical characterization of the MEA prepared by either the CCS or the CCM method suggests that the CCM is preferable because improvements in ionic conductivity far outweigh any improvements in electronic conductivity. There are few studies of degradation mechanisms that link to MEA preparation methods. A review of AEM water electrolysis performance highlights the importance of liquid electrolyte used. Pure water feeds result in poor current densities while 1%  $K_2CO_3$  or dilute KOH solutions give good results. A review of the literature results in the best performance with PGM-free catalysts (Ni-Fe, Ni-Mo, Ni/(CeO<sub>2</sub>-La<sub>2</sub>O<sub>3</sub>)/C and Cu<sub>x</sub>Co<sub>3-x</sub>O<sub>4</sub>) and a commercial membrane (Tokuyama A201). The best electrolysis performance recorded was 500 mA cm<sup>-2</sup> at 1.95 V at 60 °C with a 1%  $K_2CO_3$  electrolyte by the Bessarabov group.<sup>54</sup> The long-term durability of AEM water electrolyser cell performance has yet to be demonstrated and is a considerable challenge. The best data show performance approaching 2000 h. A clear understanding of the source(s) of degradation mechanisms (membrane, ionomer, catalyst or MEA) would help in developing more stable performance.

## 8. Conclusions and recommendations

To date, the development of catalysts, membranes and ionomers for AEM electrolysis has been sporadic with little research on integration of the various components in MEAs and cell testing. As a result the best performance data shown in AEM cells has been obtained with commercially available materials. Hence, the development of these critical components of this technology requires a future road map for systematic development and commercialization of AEM systems and components. This should include the coordination of basic and applied research, technology development & integration, and testing at a laboratory scale of small demonstration units (AEM electrolyzer short stacks) that can be used to validate the technology.

## Conflicts of interest

There are no conflicts to declare.

## Acknowledgements

The authors acknowledge Ente Cassa di Risparmio di Firenze for funding (project EnergyLab) and the PRIN 2017 Project funded by the Italian Ministry MUIR Italy (No. 2017YH9MRK). The financial support of this research received from the Ministry of Industry and Trade of the Czech Republic under project No. FV10529 is gratefully acknowledged.

## Notes and references

1 P. Nikolaidis and A. Poullikkas, *Renewable Sustainable Energy Rev.*, 2017, **67**, 597–611.

- 2 M. Momirlan and T. Veziroglu, *Renewable Sustainable Energy Rev.*, 1999, **3**, 219–231.
- 3 P. E. Dodds and S. Demoullin, *Int. J. Hydrogen Energy*, 2013, **38**, 7189–7200.
- 4 P. E. Dodds, L. Staffell, A. D. Hawkes, F. Li, P. Grunewald, W. McDowall and P. Ekins, *Int. J. Hydrogen Energy*, 2015, **40**, 2065–2083.
- 5 T. A. Napp, A. Gambhir, T. P. Hills, N. Florin and P. S. Fennell, *Renewable Sustainable Energy Rev.*, 2014, **30**, 616–640.
- 6 J. Tollefson, *Nature*, 2010, **464**, 1262–1264.
- 7 A. Midilli, M. Ay, I. Dincer and M. A. Rosen, *Renewable Sustainable Energy Rev.*, 2005, **9**, 255–271.
- 8 A. Midilli, M. Ay, I. Dincer and M. A. Rosen, *Renewable Sustainable Energy Rev.*, 2005, **9**, 273–287.
- 9 A. Demirbas, *Energy Sources, Part B*, 2017, **12**, 172–181.
- 10 R. Shandarr, C. A. Trudewind and P. Zapp, *J. Cleaner Prod.*, 2014, **85**, 151–163.
- 11 I. Staffell, D. Scamman, A. V. Abad, P. Balcombe, P. E. Dodds, P. Ekins, N. Shah and K. R. Ward, *Energy Environ. Sci.*, 2019, **12**, 463–491.
- 12 J. O. M. Bockris, *Int. J. Hydrogen Energy*, 2013, **38**, 2579–2588.
- 13 A. Ursua, E. L. Barrios, J. Pascual, I. S. Martin and P. Sanchis, *Int. J. Hydrogen Energy*, 2016, **41**, 12852–12861.
- 14 J. G. G. Clua, R. J. Mantz and H. De Battista, *Appl. Energy*, 2011, **88**, 1857–1863.
- 15 A. Kovac, D. Marcius and L. Budin, *Int. J. Hydrogen Energy*, 2019, **44**, 9841–9848.
- 16 A. Buttler and H. Spliethoff, *Renewable Sustainable Energy Rev.*, 2018, **82**, 2440–2454.
- 17 K. Zeng and D. K. Zhang, *Prog. Energy Combust. Sci.*, 2011, **37**, 631.
- 18 M. Schalenbach, O. Kasian and K. J. J. Mayrhofer, *Int. J. Hydrogen Energy*, 2018, **43**, 11932–11938.
- 19 [https://www.hydrogen.energy.gov/annual\\_review19\\_h2fuel.html#electrolysis](https://www.hydrogen.energy.gov/annual_review19_h2fuel.html#electrolysis).
- 20 <https://www.fch.europa.eu/page/call-2019>.
- 21 C. C. Pavel, F. Cecconi, C. Emiliani, S. Santiccioli, A. Scaffidi, S. Catanorchi and M. Comotti, *Angew. Chem., Int. Ed.*, 2014, **53**, 1378–1381.
- 22 J. Parrondo, C. G. Arges, M. Niedzwiecki, E. B. Anderson, K. E. Ayers and V. Ramani, *RSC Adv.*, 2014, **4**, 9875–9879.
- 23 G. Gardner, J. Al-Sharab, N. Danilovic, Y. B. Go, K. Ayers, M. Greenblatt and G. C. Dismukes, *Energy Environ. Sci.*, 2016, **9**, 184–192.
- 24 J. Durst, A. Siebel, C. Simon, F. Hasche, J. Herranz and H. A. Gasteiger, *Energy Environ. Sci.*, 2014, **7**, 2255–2260.
- 25 W. C. Sheng, H. A. Gasteiger and Y. Shao-Horn, *J. Electrochem. Soc.*, 2010, **157**, B1529–B1536.
- 26 D. Strmenik, P. P. Lopes, B. Genorio, V. R. Stamenkovic and N. M. Markovic, *Nano Energy*, 2016, **29**, 29–36.
- 27 R. Subbaraman, D. Tripkovic, K. C. Chang, D. Strmenik, A. P. Paulikas, P. Hirunsit, M. Chan, J. Greeley, V. Stamenkovic and N. M. Markovic, *Nat. Mater.*, 2012, **11**, 550–557.
- 28 C. L. Hu, L. Zhang and J. L. Gong, *Energy Environ. Sci.*, 2019, **12**, 2620–2645.



29 E. S. Liu, J. K. Li, L. Jiao, H. T. T. Doan, Z. Y. Liu, Z. P. Zhao, Y. Huang, K. M. Abraham, S. Mukerjee and Q. Y. Jia, *J. Am. Chem. Soc.*, 2019, **141**, 3232–3239.

30 X. Wu and K. Scott, *J. Power Sources*, 2012, **214**, 124–129.

31 S. H. Ahn, B. S. Lee, I. Choi, S. J. Yoo, H. J. Kim, E. Cho, D. Henkensmeier, S. W. Nam, S. K. Kim and J. H. Jang, *Appl. Catal., B*, 2014, **154**, 197–205.

32 J. Y. Huot, M. L. Trudeau and R. Schulz, *J. Electrochem. Soc.*, 1991, **138**, 1316–1321.

33 L. Xiao, S. Zhang, J. Pan, C. X. Yang, M. L. He, L. Zhuang and J. T. Lu, *Energy Environ. Sci.*, 2012, **5**, 7869–7871.

34 X. Tang, L. Xiao, C. X. Yang, J. T. Lu and L. Zhuang, *Int. J. Hydrogen Energy*, 2014, **39**, 3055–3060.

35 R. B. Patil, A. Mantri, S. D. House, J. C. Yang and J. R. McKone, *ACS Appl. Energy Mater.*, 2019, **2**, 2524–2533.

36 F. Juarez, D. Salmazo, P. Quaino and W. Schmickler, *Electrocatalysis*, 2019, **10**, 584–590.

37 A. G. Oshchepkov, A. Bonnefont and E. R. Savinova, *Electrocatalysis*, 2019, 133–142.

38 Y. Y. Chen, Y. Zhang, X. Zhang, T. Tang, H. Luo, S. Niu, Z. H. Dai, L. J. Wan and J. S. Hu, *Adv. Mater.*, 2017, **29**, 170331–170338.

39 J. Zhang, T. Wang, P. Liu, Z. Q. Liao, S. H. Liu, X. D. Zhuang, M. W. Chen, E. Zschech and X. L. Feng, *Nat. Commun.*, 2017, **8**, 15437–15445.

40 Y. S. Jin, H. T. Wang, J. J. Li, X. Yue, Y. J. Han, P. K. Shen and Y. Cui, *Adv. Mater.*, 2016, **28**, 3785–3790.

41 M. Gong, W. Zhou, M. C. Tsai, J. G. Zhou, M. Y. Guan, M. C. Lin, B. Zhang, Y. F. Hu, D. Y. Wang, J. Yang, S. J. Pennycook, B. J. Hwang and H. J. Dai, *Nat. Commun.*, 2014, **5**, 4695–4701.

42 H. Dau, C. Limberg, T. Reier, M. Risch, S. Roggan and P. Strasser, *ChemCatChem*, 2010, **2**, 724–761.

43 M. Zhang, M. de Respinis and H. Frei, *Nat. Chem.*, 2014, **6**, 362–367.

44 I. Vincent and D. Bessarabov, *Renewable Sustainable Energy Rev.*, 2018, **81**, 1690–1704.

45 S. Klaus, M. W. Louie, L. Trotochaud and A. T. Bell, *J. Phys. Chem. C*, 2015, **119**, 18303–18316.

46 F. D. Speck, K. E. Dettelbach, R. S. Sherbo, D. A. Salvatore, A. X. Huang and C. P. Berlinguet, *Chem.*, 2017, **2**, 590–597.

47 Y. J. Leng, G. Chen, A. J. Mendoza, T. B. Tighe, M. A. Hickner and C. Y. Wang, *J. Am. Chem. Soc.*, 2012, **134**, 9054–9057.

48 L. Trotochaud, S. L. Young, J. K. Ranney and S. W. Boettcher, *J. Am. Chem. Soc.*, 2014, **136**, 6744–6753.

49 J. Y. C. Chen, L. N. Dang, H. F. Liang, W. L. Bi, J. B. Gerken, S. Jin, E. E. Alp and S. S. Stahl, *J. Am. Chem. Soc.*, 2015, **137**, 15090–15093.

50 D. Gonzalez-Flores, K. Klingan, P. Chernev, S. Loos, M. R. Mohammadi, C. Pasquini, P. Kubella, I. Zaharieva, R. D. L. Smith and H. Dau, *Sustainable Energy Fuels*, 2018, **2**, 1986–1994.

51 R. D. L. Smith, C. Pasquini, S. Loos, P. Chernev, K. Klingan, P. Kubella, M. R. Mohammadi, D. Gonzalez-Flores and H. Dau, *Energy Environ. Sci.*, 2018, **11**, 2476–2485.

52 M. Gorlin, P. Chernev, P. Paciok, C. W. Tai, J. Ferreira de Araujo, T. Reier, M. Heggen, R. Dunin-Borkowski, P. Strasser and H. Dau, *Chem. Commun.*, 2019, **55**, 818–821.

53 D. Y. Xu, M. B. Stevens, M. R. Cosby, S. Z. Oener, A. M. Smith, L. J. Enman, K. E. Ayers, C. B. Capuano, J. N. Renner, N. Danilovic, Y. G. Li, H. Z. Wang, Q. H. Zhang and S. W. Boettcher, *ACS Catal.*, 2019, **9**, 7–15.

54 I. Vincent, A. Kruger and D. Bessarabov, *Int. J. Electrochem. Sci.*, 2018, **13**, 11347–11358.

55 I. Vincent, A. Kruger and D. Bessarabov, *Int. J. Hydrogen Energy*, 2017, **42**, 10752–10761.

56 X. Wu and K. Scott, *J. Mater. Chem.*, 2011, **21**, 12344–12351.

57 X. Wu, K. Scott, F. Xie and N. Alford, *J. Power Sources*, 2014, **246**, 225–231.

58 T. Pandiarajan, L. J. Berchmans and S. Ravichandran, *RSC Adv.*, 2015, **5**, 34100–34108.

59 G. Gupta, K. Scott and M. Mamlouk, *J. Power Sources*, 2018, **375**, 387–396.

60 L. Zeng, T. S. Zhao, R. H. Zhang and J. B. Xu, *Electrochem. Commun.*, 2018, **87**, 66–70.

61 R. I. Masel, Z. Liu and S. D. Sajjad, *Polym. Electrolyte Fuel Cells*, 2016, **75**(16), 1143–1146.

62 J. R. Varcoe, P. Atanassov, D. R. Dekel, A. M. Herring, M. A. Hickner, P. A. Kohl, A. R. Kucernak, W. E. Mustain, K. Nijmeijer, K. Scott, T. Xu and L. Zhuang, *Energy Environ. Sci.*, 2014, **7**, 3135–3191.

63 C. Vogel and J. Meier-Haack, *Desalination*, 2014, **342**, 156–174.

64 J. R. Varcoe and R. C. T. Slade, *Fuel Cells*, 2005, **5**, 187–200.

65 J. B. Edson, C. S. Macomber, B. S. Pivovar and J. M. Boncella, *J. Membr. Sci.*, 2012, **399–400**, 49–59.

66 D. G. Li, I. Matanovic, A. S. Lee, E. J. Park, C. Fujimoto, H. T. Chung and Y. S. Kim, *ACS Appl. Mater. Interfaces*, 2019, **11**, 9696–9701.

67 J. Ran, L. Wu, Y. He, Z. Yang, Y. Wang, C. Jiang, L. Ge, E. Bakangura and T. Xu, *J. Membr. Sci.*, 2017, **522**, 267–291.

68 K. F. L. Hagesteijn, S. Jiang and B. P. Ladewig, *J. Mater. Sci.*, 2018, **53**, 11131–11150.

69 M. A. Hickner, A. M. Herring and E. B. Coughlin, *J. Polym. Sci., Part B: Polym. Phys.*, 2013, **51**, 1727–1735.

70 G. Merle, M. Wessling and K. Nijmeijer, *J. Membr. Sci.*, 2011, **377**, 1–35.

71 G. Couture, A. Alaaeddine, F. Boschet and B. Ameduri, *Prog. Polym. Sci.*, 2011, **36**, 1521–1557.

72 Y. J. Wang, J. Qiao, R. Baker and J. Zhang, *Chem. Soc. Rev.*, 2013, **42**, 5768–5787.

73 S. Gu, B. J. Xu and Y. S. Yan, in *Annual Review of Chemical and Biomolecular Engineering*, Vol 5, ed. J. M. Prausnitz, M. F. Doherty and R. A. Segalman, Annual Reviews, Palo Alto, 2014, vol. 5, pp. 429–454.

74 M. Paidar, V. Fateev and K. Bouzek, *Electrochim. Acta*, 2016, **209**, 737–756.

75 M. Bodner, A. Hofer and V. Hacker, *WIREs Energy Environ.*, 2015, **4**, 365–381.

76 D. Hellwinkel and H. Seifert, *Liebigs Ann. Chem.*, 1972, **762**, 29–54.



77 M. G. Marino and K. D. Kreuer, *ChemSusChem*, 2015, **8**, 513–523.

78 L. Gu, H. Dong, Z. Sun, Y. Li and F. Yan, *RSC Adv.*, 2016, **6**, 94387–94398.

79 C. Vogel, H. Komber and J. Meier-Haack, *React. Funct. Polym.*, 2017, **117**, 34–42.

80 J. S. Olsson, T. H. Pham and P. Jannasch, *J. Membr. Sci.*, 2019, **578**, 183–195.

81 T. H. Pham, J. S. Olsson and P. Jannasch, *J. Mater. Chem. A*, 2018, **6**, 16537–16547.

82 J. S. Olsson, T. H. Pham and P. Jannasch, *Adv. Funct. Mater.*, 2018, **28**, 10.

83 T. H. Pham, J. S. Olsson and P. Jannasch, *J. Am. Chem. Soc.*, 2017, **139**, 2888–2891.

84 J. S. Olsson, T. H. Pham and P. Jannasch, *Macromolecules*, 2017, **50**, 2784–2793.

85 H. S. Dang and P. Jannasch, *J. Mater. Chem. A*, 2016, **4**, 11924–11938.

86 T. H. Pham and P. Jannasch, *ACS Macro Lett.*, 2015, **4**, 1370–1375.

87 H. S. Dang and P. Jannasch, *J. Mater. Chem. A*, 2016, **4**, 17138–17153.

88 H. S. Dang and P. Jannasch, *J. Mater. Chem. A*, 2017, **5**, 21965–21978.

89 D. J. Strasser, B. J. Graziano and D. M. Knauss, *J. Mater. Chem. A*, 2017, **5**, 9627–9640.

90 N. Chen, C. Lu, Y. Li, C. Long and H. Zhu, *J. Membr. Sci.*, 2019, **572**, 246–254.

91 X. M. Chu, Y. Shi, L. Liu, Y. D. Huang and N. W. Li, *J. Mater. Chem. A*, 2019, **7**, 7717–7727.

92 L. A. Diaz, R. E. Coppola, G. C. Abuin, R. Escudero-Cid, D. Herranz and P. Ocon, *J. Membr. Sci.*, 2017, **535**, 45–55.

93 L. A. Diaz, J. Hnat, N. Heredia, M. M. Bruno, F. A. Viva, M. Paidar, H. R. Corti, K. Bouzek and G. C. Abuin, *J. Power Sources*, 2016, **312**, 128–136.

94 A. Marinkas, I. Struzynska-Piron, Y. Lee, A. Lim, H. S. Park, J. H. Jang, H. J. Kim, J. Kim, A. Maljusch, O. Conradi and D. Henkensmeier, *Polymer*, 2018, **145**, 242–251.

95 A. Konovalova, H. Kim, S. Kim, A. Lim, H. S. Park, M. R. Kraglund, D. Aili, J. H. Jang, H. J. Kim and D. Henkensmeier, *J. Membr. Sci.*, 2018, **564**, 653–662.

96 J. Hnat, M. Paidar, J. Schauer and K. Bouzek, *Int. J. Hydrogen Energy*, 2014, **39**, 4779–4787.

97 J. Hnat, M. Plevova, J. Zitka, M. Paidar and K. Bouzek, *Electrochim. Acta*, 2017, **248**, 547–555.

98 J. Zitka, J. Peter, B. Galajdova, L. Pavlovec, Z. Pientka, M. Paidar, J. Hnat and K. Bouzek, *Desalin. Water Treat.*, 2019, **142**, 90–97.

99 J. Hnat, M. Paidar, J. Schauer, J. Zitka and K. Bouzek, *J. Appl. Electrochem.*, 2011, **41**, 1043–1052.

100 J. Hnat, M. Paidar, J. Schauer, J. Zitka and K. Bouzek, *J. Appl. Electrochem.*, 2012, **42**, 545–554.

101 D. D. Tham and D. Kim, *J. Membr. Sci.*, 2019, 139–149.

102 N. Lee, D. T. Duong and D. Kim, *Electrochim. Acta*, 2018, **271**, 150–157.

103 D. Aili, A. G. Wright, M. R. Kraglund, K. Jankova, S. Holdcroft and J. O. Jensen, *J. Mater. Chem. A*, 2017, **5**, 5055–5066.

104 M. R. Kraglund, D. Aili, K. Jankova, E. Christensen, Q. Li and J. O. Jensen, *J. Electrochem. Soc.*, 2016, **163**, F3125–F3131.

105 P. Häussinger, R. Lohmüller and A. M. Watson, in *Ullmann's Encyclopedia of Industrial Chemistry*, Wiley-VCH Verlag GmbH & Co. KGaA, 2000.

106 H. Ito, N. Kawaguchi, S. Someya and T. Munakata, *Electrochim. Acta*, 2019, **297**, 188–196.

107 X. Wu and K. Scott, *J. Power Sources*, 2012, **214**, 124–129.

108 L. Xiao, S. Zhang, J. Pan, C. Yang, M. He, L. Zhuang and J. Lu, *Energy Environ. Sci.*, 2012, **5**, 7869–7871.

109 N. V. Kuleshov, V. N. Kuleshov, S. A. Dovbysh, S. A. Grigoriev, S. V. Kurochkin and P. Millet, *Int. J. Hydrogen Energy*, 2019, 29441–29449.

110 J. Hnát, R. Kodým, K. Denk, M. Paidar, J. Zitka and K. Bouzek, *Chem.-Ing.-Tech.*, 2019, **91**, 821–832.

111 S. H. Ahn, S. J. Yoo, H. J. Kim, D. Henkensmeier, S. W. Nam, S. K. Kim and J. H. Jang, *Appl. Catal., B*, 2016, **180**, 674–679.

112 S. H. Ahn, B. S. Lee, I. Choi, S. J. Yoo, H. J. Kim, E. Cho, D. Henkensmeier, S. W. Nam, S. K. Kim and J. H. Jang, *Appl. Catal., B*, 2014, **154–155**, 197–205.

113 A. Lim, H. J. Kim, D. Henkensmeier, S. Jong Yoo, J. Young Kim, S. Young Lee, Y. E. Sung, J. H. Jang and H. S. Park, *J. Ind. Eng. Chem.*, 2019, **76**, 410–418.

114 H. Ito, N. Kawaguchi, S. Someya, T. Munakata, N. Miyazaki, M. Ishida and A. Nakano, *Int. J. Hydrogen Energy*, 2018, **43**, 17030–17039.

115 S. Vengatesan, S. Santhi, S. Jeevanantham and G. Sozhan, *J. Power Sources*, 2015, **284**, 361–368.

116 H. Ito, N. Miyazaki, S. Sugiyama, M. Ishida, Y. Nakamura, S. Iwasaki, Y. Hasegawa and A. Nakano, *J. Appl. Electrochem.*, 2018, **48**, 305–316.

117 A. Marinkas, I. Stružynska-Piron, Y. Lee, A. Lim, H. S. Park, J. H. Jang, H. J. Kim, J. Kim, A. Maljusch, O. Conradi and D. Henkensmeier, *Polymer*, 2018, **145**, 242–251.

118 M. K. Cho, H. Y. Park, H. J. Lee, H. J. Kim, A. Lim, D. Henkensmeier, S. J. Yoo, J. Y. Kim, S. Y. Lee, H. S. Park and J. H. Jang, *J. Power Sources*, 2018, **382**, 22–29.

119 M. K. Cho, H. Y. Park, S. Choe, S. J. Yoo, J. Y. Kim, H. J. Kim, D. Henkensmeier, S. Y. Lee, Y. E. Sung, H. S. Park and J. H. Jang, *J. Power Sources*, 2017, **347**, 283–290.

120 X. Chu, Y. Shi, L. Liu, Y. Huang and N. Li, *J. Mater. Chem. A*, 2019, **7**, 7717–7727.

121 S. Seetharaman, R. Balaji, K. Ramya, K. S. Dhathathreyan and M. Velan, *Int. J. Hydrogen Energy*, 2013, **38**, 14934–14942.

122 C. C. Pavel, F. Ceconni, C. Emiliani, S. Santiccioli, A. Scaffidi, S. Catanorchi and M. Comotti, *Angew. Chem., Int. Ed.*, 2014, **53**, 1378–1381.

123 G. C. Chen, T. H. Wondimu, H. C. Huang, K. C. Wang and C. H. Wang, *Int. J. Hydrogen Energy*, 2019, **44**, 10174–10181.

124 E. López-Fernández, J. Gil-Rostra, J. P. Espinós, A. R. González-Elipe, F. Yubero and A. de Lucas-Consuegra, *J. Power Sources*, 2019, **415**, 136–144.

125 B. K. Kakati, D. Sathiyamoorthy and A. Verma, *Int. J. Hydrogen Energy*, 2010, **35**, 4185–4194.



126 Z. Liu, S. D. Sajjad, Y. Gao, H. Yang, J. J. Kaczur and R. I. Masel, *Int. J. Hydrogen Energy*, 2017, **42**, 29661–29665.

127 D. Aili, M. K. Hansen, J. W. Andreasen, J. Zhang, J. O. Jensen, N. J. Bjerrum and Q. Li, *J. Membr. Sci.*, 2015, **493**, 589–598.

128 W. Ju, M. V. F. Heinz, L. Pusterla, M. Hofer, B. Fumey, R. Castiglioni, M. Pagani, C. Battaglia and U. F. Vogt, *ACS Sustainable Chem. Eng.*, 2018, **6**, 4829–4837.

129 E. J. Park, C. B. Capuano, K. E. Ayers and C. Bae, *J. Power Sources*, 2018, **375**, 367–372.

130 L. Wang, T. Weissbach, R. Reissner, A. Ansar, A. S. Gago, S. Holdcroft and K. A. Friedrich, *ACS Appl. Energy Mater.*, 2019, **2**, 7903–7912.

131 J. Hnát, M. Plevova, R. A. Tufa, J. Zitka, M. Paidar and K. Bouzek, *Int. J. Hydrogen Energy*, 2019, **44**, 17493–17504.

132 Y. Leng, G. Chen, A. J. Mendoza, T. B. Tighe, M. A. Hickner and C. Y. Wang, *J. Am. Chem. Soc.*, 2012, **134**, 9054–9057.

133 X. Wu and K. Scott, *J. Power Sources*, 2012, **206**, 14–19.

134 X. Wu and K. Scott, *Int. J. Hydrogen Energy*, 2013, **38**, 3123–3129.

135 J. E. Park, S. Y. Kang, S. H. Oh, J. K. Kim, M. S. Lim, C. Y. Ahn, Y. H. Cho and Y. E. Sung, *Electrochim. Acta*, 2019, **295**, 99–106.

136 X. Su, L. Gao, L. Hu, N. A. Qaisrani, X. Yan, W. Zhang, X. Jiang, X. Ruan and G. He, *J. Membr. Sci.*, 2019, 283–292.

137 X. Liang, G. Pan, L. Xu and J. Wang, *Fuel*, 2015, **139**, 393–400.

138 V. Vijayakumar and S. Y. Nam, *J. Ind. Eng. Chem.*, 2019, **70**, 70–86.

139 X. Wu and K. Scott, *J. Mater. Chem.*, 2011, **21**, 12344–12351.

140 Y. C. Cao, X. Wu and K. Scott, *Int. J. Hydrogen Energy*, 2012, **37**, 9524–9528.

141 L. Zeng and T. S. Zhao, *Nano Energy*, 2015, **11**, 110–118.

142 G. Borisov, H. Penchev, K. Maksimova-Dimitrova, F. Ublekov, E. Lefterova, V. Sinigersky and E. Slavcheva, *Mater. Lett.*, 2019, **240**, 144–146.

143 M. Faraj, M. Boccia, H. Miller, F. Martini, S. Borsacchi, M. Geppi and A. Pucci, *Int. J. Hydrogen Energy*, 2012, **37**, 14992–15002.

144 J. Žitka, M. Bleha, J. Schauer, B. Galajdová, M. Paidar, J. Hnát and K. Bouzek, *Desalin. Water Treat.*, 2015, **56**, 3167–3173.

145 L. A. Diaz, J. Hnát, N. Heredia, M. M. Bruno, F. A. Viva, M. Paidar, H. R. Corti, K. Bouzek and G. C. Abuin, *J. Power Sources*, 2016, **312**, 128–136.

146 J. Hnát, M. Plevová, J. Žitka, M. Paidar and K. Bouzek, *Electrochim. Acta*, 2017, **248**, 547–555.

147 L. S. Darken and H. F. Meier, *J. Am. Chem. Soc.*, 1942, **64**, 621–623.

148 C. Thieme, in *Ullmann's Encyclopedia of Industrial Chemistry*, 2012.

149 H. Schultz, in *Ullmann's Encyclopedia of Industrial Chemistry*, 2000.

150 M. Schalenbach, A. R. Zeradjanin, O. Kasian, S. Cherevko and K. J. J. Mayrhofer, *Int. J. Electrochem. Sci.*, 2018, **13**, 1173–1226.

151 J. Hnát, M. Paidar, J. Schauer and K. Bouzek, *Int. J. Hydrogen Energy*, 2014, **39**, 4779–4787.

152 S. Suzuki, H. Muroyama, T. Matsui and K. Eguchi, *Electrochim. Acta*, 2013, **88**, 552–558.

153 F. Helfferich, *Ion exchange*, Dover publications, Inc., New York, 1995.

154 B. Beverskog and I. Puigdomenech, *Corros. Sci.*, 1997, **39**, 969–980.

155 J. Schauer, J. Hnát, L. Brožová, J. Žitka and K. Bouzek, *J. Membr. Sci.*, 2015, **473**, 267–273.

156 D. Chanda, J. Hnát, T. Bystron, M. Paidar and K. Bouzek, *J. Power Sources*, 2017, **347**, 247–258.

157 D. Chanda, J. Hnát, A. S. Dobrota, I. A. Pašti, M. Paidar and K. Bouzek, *Phys. Chem. Chem. Phys.*, 2015, **17**, 26864–26874.

158 D. Chanda, J. Hnát, M. Paidar and K. Bouzek, *Int. J. Hydrogen Energy*, 2014, **39**, 5713–5722.

159 D. Chanda, J. Hnát, M. Paidar, J. Schauer and K. Bouzek, *J. Power Sources*, 2015, **285**, 217–226.

160 W. Ju, M. V. F. Heinz, L. Pusterla, M. Hofer, B. Fumey, R. Castiglioni, M. Pagani, C. Battaglia and U. F. Vogt, *ACS Sustainable Chem. Eng.*, 2018, **6**, 4829–4837.

161 M. Ďurovič, J. Hnát, C. I. Bernäcker, T. Rauscher, L. Röntzsch, M. Paidar and K. Bouzek, *Electrochim. Acta*, 2019, **306**, 688–697.

162 D. R. Dekel, I. G. Rasin and S. Brandon, *J. Power Sources*, 2019, **420**, 118–123.

163 Y. X. Chen, A. Lavacchi, H. A. Miller, M. Bevilacqua, J. Filippi, M. Innocenti, A. Marchionni, W. Oberhauser, L. Wang and F. Vizza, *Nat. Commun.*, 2014, **5**, 4036–4042.

164 Y.-K. Choe, C. Fujimoto, K.-S. Lee, L. T. Dalton, K. Ayers, N. J. Henson and Y. S. Kim, *Chem. Mater.*, 2014, **26**, 5675–5682.

165 C. Fujimoto, D.-S. Kim, M. Hibbs, D. Wroblewski and Y. S. Kim, *J. Membr. Sci.*, 2012, **423–424**, 438–449.

166 A. D. Mohanty, S. E. Tignor, J. A. Krause, Y.-K. Choe and C. Bae, *Macromolecules*, 2016, **49**, 3361–3372.

167 K. M. Meek, J. R. Nykaza and Y. A. Elabd, *Macromolecules*, 2016, **49**, 3382–3394.

168 W. You, K. J. T. Noonan and G. W. Coates, *Prog. Polym. Sci.*, 2020, **100**, 101177.

